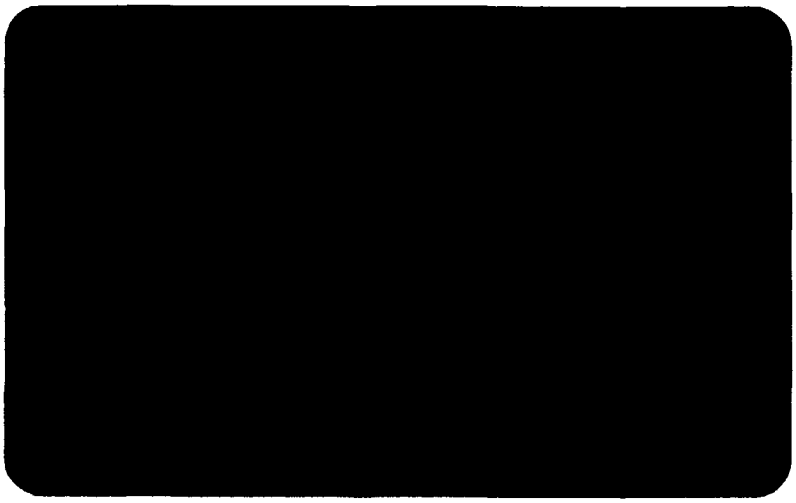

TU Delft

MEMORANDUM M-667

An Experimental study of the angled crack in GLARE 3

K.J.J.M. Zaal

April, 1993

Delft University of Technology
Faculty of Aerospace Engineering
Delft, The Netherlands

Abstract

The aim of the present investigation is to perform both an experimental and a theoretical study of the behaviour of cracks in GLARE loaded under a combined mode I and mode II loading, using the angled crack problem. Cracks originating from impact damage in aircraft fuselages can experience a mixed mode I and II load at the start of their life. For GLARE, the more fibrous nature of GLARE compared to aluminium may change the propagation. The experiments were performed on specimens made of GLARE-3, with the main material directions aligned with the specimen axis. As reference materials, both aluminium 2024-T3 and 7075-T6 are used. For angled cracks, the propagation direction has been predicted by Erdogan and Sih, Williams and Ewing and Theocaris *et al.*

The failure load increased with increasing crack tilt angle for all the studied materials. For Al 7075-T6 and GLARE-3, also the nett-section stress at failure increased. All models seem to predict similar crack propagation directions. The model of Williams and Ewing seems to perform best in predicting the variation in failure load, mainly due to the one free variable in it. For Al 2024-T3 the nett section yield criterion did as well as the model of Williams and Ewing. GLARE-3 does not seem to be as sensitive to nett-section yield as AL 2024-T3, nor does it seem to be as brittle as Al 7075-T6.

The model of Williams and Ewing does not explain the size effects found in residual strength experiments. The T-criterion of Theocaris *et al.* would show the influence of the T-stress on the plastic zone and thus attempt to model the size effect, but does not seem to work for the present specimens. The model of Williams and Ewing was used by Finnie and Saith to model the path stability of cracks. Since however the angled crack and the path unstable crack differ in propagation mode, both might not be governed by the same value of the variable r_c.

Since the Westergaard equations do not seem to be valid at the crack tip within the linear theory of elasticity, the elastic models based on these equations may only be valid in a similarity approach. Than, the variable r_c in the model of Williams and Ewing and Finnie and Saith would indicate a fictitious radius indicating the balance between the influence of the stress intensities and the T-stress on crack propagation.

Table of contents

List of symbols

a	half crack length [mm]
E	Young's modulus [MPa]
G	shear modulus [MPa]
K	stress intensity factor [$MPa\sqrt{mm}$]
r,θ	local polar coordinates at the crack tip
r, a	orthotropic material constants
s_1,s_2	orthotropic complex material constants
s'_1,s'_2	anisotropic complex material constants
t	plate thickness [mm]
P	external load [kN]
r_c	material failure radius in Williams' and Ewing's model [mm]
T	strain energy density
T	T-stress [MPa]
W	width [mm]
x,y	local cartesian coordinates at the crack tip
α	crack tilt angle in the uni-directionally loaded plate, relative to the position perpendicular to the main loading [°]
ν	Poisson's ratio
ψ_i	root of complex coordinates $x + s_i y$
σ	tensile stress [MPa]
τ	shear stress [MPa]
Subscripts	
al	aluminium
D	distortional part of the strain energy density
fail	experimental specimen failure
I,II	with respect to a mode II and II type of deformation around the crack tip
lig	unbroken ligament
nett	with respect to the nett section formed by the unbroken ligaments
pl	plastic
pred	predicted
ult	ultimate
V	dilatanional part of the strain energy density
0.2	0.2% off-set yield stress

List of tables

List of figures

1 Introduction

Cracks usually are assumed to grow under a mode I loading only. Especially fatigue cracks will hardly ever experience a mode II loading between initiation and final static failure. Cracks originating from impact damage however can experience a mixed mode I and II load at the start of their life. The direction of an impact crack with respect to the loading situation is quite arbitrary. In general, a through crack perpendicular to the largest internal load in the structure will give the lowest residual strength. A so called "angled" crack (figure 1.1), with a position tilted from the generally most serious position perpendicular to the main load, will usually have a higher residual strength. The angle under which the angled crack will propagate, has been predicted i.e by Williams and Ewing [1,2] and Theocaris *et al.* [3,4]. For GLARE [5], studying the angled crack may be of importance for two questions. Firstly, the more fibrous nature of GLARE compared to aluminium may change the propagation angle of the angled crack and thus the residual strength of impact damage. Secondly, Finnie and Saith [6] applied the criterion of Williams and Ewing to predict the crack path stability of cracks. The crack path stability of cracks in fuselages [7] might thus be linked to the angled crack problem.

The aim of the present investigation is to perform both an experimental and a theoretical study of the behaviour of cracks in GLARE loaded under a combined mode I and mode I loading, using the angled crack. For the specimens made of GLARE-3, the main material directions are aligned with the specimen axis, not with the crack axis. As reference materials, both aluminium 2024-T3 and 7075-T6 are used. Aluminium 2024-T3 would be the counterpart of GLARE-3 as a possible fuselage material [8]. Aluminium 7075-T6 would form the scientific bench mark as a material sensitive to stress intensity factors.

The experimentally obtained crack propagation directions and failure loads will be compared to predictions from the nett-section yield criterion, the maximum tensile hoop stress criterion of Erdogan and Sih [9], the maximum tensile hoop stress criterion of Williams and Ewing and the T-criterion of Theocaris *et al.*

2 Experiments

The present experiments were performed on specimens with a central angled crack, with varying crack tilt angle. The specimens were made of aluminium 7075-T6, aluminium 2024-T3 and GLARE-3. They were loaded under constant increasing end-displacement. The failure load was recorded and the shape of the crack propagation studied. These subjects will be discussed in somewhat more detail in this chapter.

2.1 Materials

In future aircraft, GLARE-3 may be a candidate as fuselage skin material [8]. It would in that function compete with among others aluminium 2024-T3. In the present experiments, GLARE-3 with a thickness of 1.4 mm is compared to aluminium 2024-T3 with a thickness of 1.6 mm, anticipating the weight gain when GLARE is used. Both materials are compared to aluminium 7075-T6 with a thickness of 1.6 mm. Aluminium 7075-T6 is to a much larger extend governed by the theory of fracture mechanics than 2024-T3 [10, figure 5.17] and would allow a more reliable comparison of fracture mechanics theories and the present experiments. The materials used in the experiments are listed in table 2.1.

2.2 Specimen design

The centrally cracked uni-directionally loaded plate was chosen as test specimen. It is easy to make and test. The specimens were 400 mm long and 160 mm wide (figure 2.1.a). On each end of the specimens, approximately 55 mm was used to clamp the specimen. The total crack length $2a$ was kept equal to 40 mm for all specimens. The cracks were located in the middle of the specimens, with a varying tilt angle compared to the position perpendicular to the loading. For each material, six specimens were tested. The tilt angle, varying from 0° to 75° in steps of 15°, was the only difference between the specimens made of one material. The main specimen dimensions and crack tilt angles are listed in table 2.2 and 2.3.

Small, drilled holes with a diameter of 0.6 mm were used as crack tips. Compared to the square crack tip as made by the blade of a saw-cut, the round hole is thought to interfere less with the propagation direction preferred by the crack. Towards the small holes, the crack was cut with a saw-cut with a blade thickness of approximately 0.35 mm, starting from a hole in the middle of the crack. In figure 2.1.b, the ideal crack tip is drawn. In all cases, the saw-cut did enter the small hole, although in many cases not symmetrically.

2.3 Test procedure

The specimens were tested under a static tensile load on an Amsler material testing machine, under end-displacement control. The specimens made of aluminium 7075-T6 were loaded with a rate of 3 mm per minute. The specimens made of aluminium 2024-T3 and GLARE-3 were loaded with a rate of 1.5 mm per minute. The maximum applied load was recorded as failure load. One crack tip was monitored with a microscope.

2.4 Failure load

For all specimens, the maximum applied load was recorded as failure load. Under force control, the maximum load would be the load at which the instable propagation of the crack would start. The failure load for the specimens is listed in table 2.4.

2.5 Shape of the crack propagation

The cracks propagated mainly in horizontal directions from the crack tips, with slight downward curves at the start (figure 2.2). The fracture surfaces in the aluminium specimens were all tilted over 45°.

3 Theories

In engineering fracture mechanics, both plastic failure criteria and elastic failure criteria are available. The elastic criteria are usually based on Westergaard-type liner elastic solutions around the crack tip. The plastic criteria are usually based on an assumed failure mode and perfectly plastic materials.

3.1 Plasticity based failure models

Nett-section yield is a well known failure model for aluminium plates with centre cracks. The model is based on the little amount of strain hardening for large amounts of plastic deformations as found e.g. in Al 2024-T3. Due to the large plastic deformation capabilities of Al 2024-T3, the entire nett-section of a centre-cracked plate can become plastic before failure. Along the nett-section, the little amount of strain-hardening will cause an almost constant stress, despite the larger variation in plastic deformation (figure 3.1). Thus, the loading on the end of the specimen can be linked to an average nett-section stress:

$$\sigma_{nett} = \frac{P_{fail}}{2tW_{lig}} \tag{3.1}$$

The nett-section yield model assumes that the specimen fails when the nett-section stress has reached some representative yield stress. For the yield stress, one cold choose e.g. the 0.2% yield stress or the ultimate stress [11]. For a normal centre cracked plate made of Al 2024-T3, the nett-section model has been found to describe the failure behaviour for varying crack lengths (see e.g. [10, figure 5.17]).

The nett-section yield model is intended for plates with a finite width only. For infinite plates, the Dugdale model [12] provides the same design opportunities. In the Dugdale model, a part of the crack ear the crack tip is assumed to be bridged by the original material in a perfectly plastic state (figure 3.2). Both models should merge when the plastic zones around the crack tip almost reaches the plate edges. However, since both models use simplifications of the plastic behaviour of the plate, this transition will not be easy to describe theoretically. The Dugdale model has been applied by Ghassem, Rich, Low and Cartwright[13,11,14] to account for the plasticity effect in the skin of a stiffened structure.

Limit analysis, known from the theory of plasticity, might suffer from the same problem. In limit analysis, slip lines are assumed on the plate (figure 3.3). After assuming a representative shear yield stress along these lines, the failure load can be linked to the material behaviour and the specimen shape. In experiments, the contraction of the plate has been found [15]. Limit analysis will not allow for a plastic zone confined within the specimens, since the slip lines must end at a plate edge.

The Dugdale model can not be used for centre cracked specimens with a tilted crack, since this would require an analytical solution of a crack with two kinks. The limit analysis might be used for centre-cracked specimens with a tilted cracks, but only for materials where the plastic zones reaches the plate edge. For such situations, the nett-section yield model will do equally

well. For centre cracked specimens with tilted cracks, the size of the unbroken ligament is equal to:

$$2W_{lig} = 2\,(W - a\cos\alpha) \tag{3.2}$$

Subsequently, the magnitude of the nett-section failure stress can be linked to the specimen failure load using equation (3.1).

For the present experiments, the nett-section failure stress has been derived and listed in table 3.1 to 3.3. As was known, aluminium 2024-T3 is sensitive to nett-section yield (see e.g. [10, figure 5.17]). In figure 3.6, the nett-section failure stress has been plotted as a function of the crack tilt angle. The stresses are normalised with the nett-section failure stress from the specimen with the 0° crack tilt angle. One may observe that for aluminium 2024-T3, all specimens failed at approximately the same nett-stress. Assuming a maximum error of 0.4 mm in the half-crack length a, a maximum error of 1.3% could be expected in the nett-section failure stress. Only the specimen with the 15° crack tilt angle is well outside this margin of error.

Aluminium 7075-T6 behaves much more brittle and for this material the stress intensity factor provides a better prediction of the failure load than for Al 2024-T3 (see e.g. [10, figure 5.17]). Especially the specimen with the 75° crack tilt angle shows a much higher nett-section failure stress than the other specimens. The specimens with the crack tilt angles in between 0° and 75°, show a continuous change of nett-section failure stress, again outside the expected margin of error. For the specimens with the 15°, 30° and 45° crack tilt angle, the nett-section failure stress is below the nett-section failure stress of the 0° specimen.

At higher crack tilt angles, the specimens made of GLARE-3 behave qualitatively similar to aluminium 7075-T6, although quantitatively the change of nett-section failure stress is much smaller. For the smaller crack tilt angles, the GLARE-3 specimens do not exceed the expected margins of error. It does not seem that GLARE-3 is as sensitive to nett-section yield as aluminium 2024-T3, nor can one say it behaves as brittle as aluminium 7075-T6.

3.2 Elasticity based failure models

Elasticity based failure models for cracked specimens start from the description of the elastic stresses around the crack tip as found first by Westergaard [16]. Hutchinson, Rice and Rosengren [17,18] included the plastic behaviour of power-hardening materials within the Westergaard-type solutions. None of the theories however takes into account the geometrical non-linearity at the crack tip (see §3.3). Since the geometrically linear Westergaard-type solutions are not valid at the crack tip, the failure models based on these equations can only serve as engineering design tool and not to study the stresses around the crack tip.

Several elasticity based models have been developed. Among them, the maximum hoop stress model of Erdogan and Sih [9], and the dilatational energy density model of Theocaris *et al.* [3,4] could be mentioned. In both models, both the stress intensity factors and the T-stress can be included. The importance of the T-stress in describing the stresses around the crack tip has been shown by e.g. [19] and Smith [20].

3.2.1 The linear elastic stress field around a crack tip

In the limit towards the crack tip, Westergaard-type solutions predict a standard stress distribution of stresses around any crack tip in an isotropic material, independent of the geometry of the crack, the geometry of the structure or type of the loading. All non-vanishing stresses around the crack tip can be quantified with three variables. Two variables - the mode I and mode II stress intensity factors K_I and K_{II} - describe the stresses that would become infinite in an ideally elastic solid. The third variable - the T-stress - describes the stresses that remain finite and constant around the crack tip. In formula form, the stresses around the crack tip can be described as:

$$\sigma_x = \frac{K_I}{\sqrt{2\pi r}}\cos\frac{\theta}{2}\left(1 - \sin\frac{\theta}{2}\sin\frac{3\theta}{2}\right) - \frac{K_{II}}{\sqrt{2\pi r}}\sin\frac{\theta}{2}\left(2 + \cos\frac{\theta}{2}\cos\frac{3\theta}{2}\right) + T \quad (3.3.a)$$

$$\sigma_y = \frac{K_I}{\sqrt{2\pi r}}\cos\frac{\theta}{2}\left(1 + \sin\frac{\theta}{2}\sin\frac{3\theta}{2}\right) + \frac{K_{II}}{\sqrt{2\pi r}}\sin\frac{\theta}{2}\cos\frac{\theta}{2}\cos\frac{3\theta}{2} \quad (3.3.b)$$

$$\tau_{xy} = \frac{K_I}{\sqrt{2\pi r}}\cos\frac{\theta}{2}\sin\frac{\theta}{2}\cos\frac{3\theta}{2} + \frac{K_{II}}{\sqrt{2\pi r}}\cos\frac{\theta}{2}\left(1 - \sin\frac{\theta}{2}\sin\frac{3\theta}{2}\right) \quad (3.3.c)$$

Here, the stresses are defined in the local cartesian coordinates at the crack tip, at a location defined in the local polar coordinate system at the crack tip (figure 1.1). Using the three variables K_I, K_{II} and T, a similarity approach will allow the comparison of cracks in different structures and under different loading. The fatigue crack growth rate is mainly governed by the mode I stress intensity factor K_I. Fatigue cracks usually grow only under a mode I loading and plastic effects are usually small enough to eliminate any influence of the T-stress. The T-stress can however have an influence on the static failure load [19] and on the shape of the crack propagation [7].

Ignoring the finite width, the stress intensity factors and T-stress for the uni-directionally loaded specimen are equal to [21]:

$$K_I = \sigma\sqrt{\pi a}\cos^2\alpha \quad (3.4.a)$$

$$K_{II} = \sigma\sqrt{\pi a}\sin 2\alpha \quad (3.4.b)$$

$$T = -\sigma\cos 2\alpha \quad (3.4.c)$$

In anisotropic solids, the same three variables can be used to describe the stress field around a crack tip. Now however, the material characteristics modify the actual shape of the stress file around the crack tip. Expressed in the theory of anisotropic plates [22, 23, 24], the stress field looks like:

$$\sigma_x = \frac{K_I}{\sqrt{2\pi r}} \mathrm{Re}\left[\frac{s_1 s_2}{s_2 - s_1}\left\{\frac{s_1}{\sqrt{\psi_1}} - \frac{s_2}{\sqrt{\psi_2}}\right\}\right] + \frac{K_{II}}{\sqrt{2\pi r}} \mathrm{Re}\left[\frac{1}{s_2 - s_1}\left\{\frac{s_1^2}{\sqrt{\psi_1}} - \frac{s_2^2}{\sqrt{\psi_2}}\right\}\right] + T \qquad (3.5.a)$$

$$\sigma_y = \frac{K_I}{\sqrt{2\pi r}} \mathrm{Re}\left[\frac{1}{s_2 - s_1}\left\{\frac{s_2}{\sqrt{\psi_1}} - \frac{s_1}{\sqrt{\psi_2}}\right\}\right] + \frac{K_{II}}{\sqrt{2\pi r}} \mathrm{Re}\left[\frac{1}{s_2 - s_1}\left\{\frac{1}{\sqrt{\psi_1}} - \frac{1}{\sqrt{\psi_2}}\right\}\right] \qquad (3.5.b)$$

$$\tau_{xy} = \frac{K_I}{\sqrt{2\pi r}} \mathrm{Re}\left[\frac{s_1 s_2}{s_2 - s_1}\left\{\frac{1}{\sqrt{\psi_2}} - \frac{1}{\sqrt{\psi_1}}\right\}\right] + \frac{K_{II}}{\sqrt{2\pi r}} \mathrm{Re}\left[\frac{1}{s_2 - s_1}\left\{\frac{s_2}{\sqrt{\psi_2}} - \frac{s_1}{\sqrt{\psi_1}}\right\}\right] \qquad (3.5.c)$$

where:

$$\psi_i = \sqrt{\cos\theta + s_i \sin\theta} \qquad (3.6.a)$$

and for orthotropic materials:

$$s_1 = \sqrt{\frac{r - a}{2}} + i\sqrt{\frac{r + a}{2}} \qquad (3.7.a)$$

$$s_2 = \sqrt{\frac{r - a}{2}} - i\sqrt{\frac{r + a}{2}} \qquad (3.7.b)$$

$$r = \sqrt{\frac{E_x}{E_y}} \qquad (3.7.c)$$

$$a = \frac{E_x}{2G_{xy}} - \upsilon_{xy} \qquad (3.7.d)$$

Similar to isotropic materials:

$$K_I = \sigma\sqrt{\pi a}\cos^2\alpha \qquad (3.8.a)$$

$$K_{II} = \sigma\sqrt{\pi a}\sin 2\alpha \qquad (3.8.b)$$

$$T = \sigma(\sin^2\alpha + \cos^2\alpha \mathrm{Re}[s_1 s_2] + \sin\alpha\cos\alpha \mathrm{Re}[s_1 + s_2]) \qquad (3.8.c)$$

In anisotropic solids, the similarity approach can only be used to compare different cracks if the occur in materials with identical material parameters s_1 and s_2.

3.2.2 Maximum hoop stress criterion

The maximum hoop stress criterion, as described e.g. by Erdogan and Sih [9], assumes that a crack will propagate in the direction where the hoop stress σ_θ around the crack tip is maximal (figure 3.4). In the equations (3.3.a) to (3.3.c), the distribution of the stresses around the crack tip is specified in the local cartesian x-y coordinate system at the crack tip. Using coordinate transformation formula's, the hoop stress in the local polar r-θ coordinate system at the crack tip can be derived:

$$\sigma_\theta = \sigma_x \sin^2\theta + \sigma_y \cos^2\theta - 2\tau_{xy} \sin\theta \cos\theta \qquad (3.9)$$

The maximum hoop stress criterion only takes into account the part of the stress distribution described by the mode I and mode II stress intensity factors K_I and K_{II}. In brittle materials, which fail at loads well below their elastic limit, these stress intensity factors would on their own describe the main part of the stresses around the crack tip. For such materials, the hoop stress criterion might yield the direction into which the crack will propagate by locating the maximum of the hoop stress in equation (3.9) with respect to the angle θ. By assuming that the propagation will start when the hoop stress reaches a critical value, one might also try to predict the failure load of the specimen. This prediction of the failure load is clearly based on an engineering approach. in the prediction, the difference between the initial onset of crack propagation and the final failure of the specimen is ignored. While equation (3.9) could be thought to describe the stresses around the crack tip up to the onset of crack propagation, a significant amount of stable tearing could both significantly change the crack shape and take the crack tip well outside the range of validity of the equations (3.3.a) to (3.3.c).

The location of the maximum hoop stress in the specimens made of Al 7075-T6 and Al 2024-T3 have been determined and listed in table 3.4 and 3.5. No comparison is made with the experimentally observed direction of crack propagation (see paragraph 4). The angle where the hoop stress becomes maximal is independent of the radial position from the crack tip. Thus, also the intensity of the maximum hoop stress with changing radial position can be determined, as listed in table 3.4 and 3.5. The intensity of the maximum hoop stress is determined for a load with the same magnitude as the failure load found in the experiments (table 3.1 and 3.2). Thus, if the maximum hoop stress criterion would be valid, all specimens should have failed at the same intensity of hoop stress. In figure 3.7, the intensity of the maximal hoop at failure in each specimen is compared to the intensity at failure in the specimen with the crack perpendicular to the loading. As can be seen, the specimens failed at decreasing intensities of the maximum hoop stress. The criterion does for the present specimens not seem to provide an engineering tool to predict the specimen failure load for the present specimens and materials.

For the GLARE-3 specimens, the same approach can be used as was used for the aluminium specimens. In GLARE too, the distribution of the hoop stress σ_θ is independent of the radial position from the crack tip if only the stresses from the mode I and mode II stress intensity factor are considered. Therefore, the hoop stress intensity can be derived using equation (3.9), once the stresses σ_x, σ_y and τ_{xy} are known from the equations (3.5.a) to (3.5.c). Similar to iso-

tropic materials, the stress intensities can be derived using equation (3.8.a) and (3.8.b). Now however, also the anisotropic material parameters s_1 an s_2 are required to obtain the magnitude of the stresses. In the equations (3.5.a) to (3.5.c), s_1 an s_2 are defined with respect to the local cartesian coordinate system at the crack tip. The evaluation of s_1 an s_2 in the equations (3.7.a) to (3.7.d) is valid only in the global X-Y specimen coordinate system, since this system coincides with the material axis defining the orthotropy of the material. Thus, they are only the orthotropic material parameters s_1 an s_2. One can however transform these easily obtained orthotropic material parameters to the required anisotropic ma parameters, with equations similar to equation (3.9). After a notation of Lekhnitskii [22]:

$$s'_1 = \frac{s_1 \cos\alpha - \sin\alpha}{\cos\alpha + s_1 \sin\alpha} \tag{3.10.a}$$

$$s'_2 = \frac{s_2 \cos\alpha - \sin\alpha}{\cos\alpha + s_2 \sin\alpha} \tag{3.10.b}$$

where s_1 and s_2 are the orthotropic material parameters from equation (3.7.a) to (3.7.d), and s'_1 and s'_2 are the anisotropic material parameters in the local x-y coordinate system at the crack tip, obtained after a rotation with a magnitude equal to the crack tilt angle α, from the global specimen system to the local crack tip system.

Using the theoretical material properties as specified in table 2.1, the magnitude and the angular position of the maximum hoop stress have been determined (table 3.6). The calculations were made with the specimens loaded by the failure stresses as found in the experiments (table 3.3). Plotting the obtained maximum hoop stresses at failure for all specimens relative to the maximum hoop stresses at failure for the specimen with the crack perpendicular to the loading (figure 3.7), one can see that also for GLARE-3 the maximum hoop stress criterion does not seem to be valid as an engineering design tool.

3.2.3 Williams' and Ewing's criterion

Besides the mode I and mode II stress intensity factors, also the T-stress has been known to have an influence on the failure load of cracked structures [19]. For materials which show plastic deformations at the crack tip before failure occurs, the T-stress can change the shape and size of the plastic zone around the crack tip, and thus change the failure load. Williams and Ewing [1,2] incorporated the T-stress in the maximum hoop stress criterion. To find the proper balance between the influence of the stress intensity factors and the T-stress, they proposed to evaluate the hoop stress at some distance r_c from the crack tip. They postulated that this distance was a material parameter. One does not have to assume that the radius r_c is a physical radius. It might be seen as a fictitious radius determining the balance between the contributions of the stress intensity factors and the T-stress to the failure load.

Finnie and Saith [6] applied Williams' and Ewing's criterion to predict the path instability of cracks. For path instability, Kosai *et al.* [25] determined that for aluminium, the material parameter r_c is equal to 1.5 mm. One can not directly assume that the magnitude of r_c which de-

termines the crack path stability is identical to the magnitude of r_c which determines the crack propagation direction for a tilted crack. For both situations, the shape of the crack propagation is different. The tilted crack propagates as a straight crack extension with a kink between the original crack and the extension. In case of crack path instability, the crack will not show a kink but instead curve from the straight crack line. However, the magnitude of 1.5 mm for r_c has been applied to study the crack propagation for the tilted cracks in the presently studied specimens. In table 3.7 and 3.8, the magnitude and the angular position of maximum hoop stress at a radius of 1.5 mm and a load equal to the experimental failure load has been determined for the aluminium specimens. As can be seen in figure 3.8, the magnitude of the maximum hoop stress at failure changes quite significantly for all specimens. One can however optimize the magnitude of r_c, in order to obtain a better prediction. As can be seen in table able 3.7 and 3.8 and figure 3.9, the scatter of the magnitude of the maximum hoop stress at failure can be reduced to 5% when for r_c a value of 1.18 and 2.95 mm is used for respectively Al 7075-T6 and Al 2024-T3. The difference in r_c for both types of aluminium may be justified by observing that both have a different plastic behaviour. For a perfectly brittle material the T-stress should not have an influence on the failure load and r_c should thus be equal to zero. Since compared to Al 2024-T3, Al 7075-T6 is much more brittle, it is not surprising it has a lower r_c.

The criterion of Williams and Ewing can be applied to GLARE-3 in two ways. Firstly, one could study the average hoop stresses in the laminate and assume that one value for r_c would describe the failure process in all layers. For this approach, one might have to assume that the failure stress varies with the crack propagation direction relative to the fibre orientation. For the present experiments however, the cracks propagated more or less into the same direction relative to the fibres.

Secondly, one could study the hoop stresses in the aluminium layers only and apply the value found for r_c as found in the Al 2024-T3 specimens. This approach would only take into account the elastic presence of the fibre layers in determining the stress distribution. Both approaches are shown in table 3.9 and figure 3.10. One can see that with an optimized magnitude of 2.01 mm for r_c, the predictions are better for the method using the average stresses than the predictions using the stresses in the aluminium layers only.

Using the presently obtained values for r_c for the presently studied materials, one may try and predict the path stability of cracks found in such structures. Since all materials have different magnitudes for r_c, the path stability of such cracks seems material dependant. Observing from the presently obtained values, the likelihood of crack path instability under equal loading seems to decline from Al 2024-T3 to GLARE-3 and to Al 7075-T6. Since such a material dependence has never been shown to exist in experiments, one can not predict whether this dependence exists, whether the values obtained for r_c in the present experiments are not valid in Finnie and Saith's criterion, whether the values obtained for r_c in the present experiments are not valid in other types of specimens or whether the criterion of Finnie and Saith may not be useable as a design tool.

3.2.4 The T-criterion of Theocaris *et al.*

The T-criterion of Theocaris *et al.* [3,4] is designed to perform similar predictions as the maximum hoop stress criterion in the previous paragraph. It predicts the angle into which a crack will propagate when it is loaded under a mixed mode loading. Similar to the maximum hoop stress criterion, it could also be used to predict crack path instability.

In the T-criterion, the energy density is used to determine the direction into which the crack will propagate. The total energy density T of a material element is split into the dilatational energy density T_v, and the distortional energy density T_D. According to Bisplinghoff *et al.* [26], the various energy density for a thin plate in plane stress can be expressed as:

$$T = \frac{1}{4G}\frac{1}{1+\nu}(\sigma_x^2+\sigma_y^2-2\nu\sigma_x\sigma_y+2(1+\nu)\tau_{xy}) \tag{3.11}$$

$$T_v = \frac{1}{18K}(\sigma_x+\sigma_y)^2 = \frac{1}{6G}\frac{1-2\nu}{2(1+\nu)} \tag{3.12}$$

$$T_D = \frac{1}{6G}(\sigma_x^2+\sigma_y^2-\sigma_x\sigma_y+3\tau_{xy}) \tag{3.13}$$

where G is the material's shear modulus and ν its Poisson's ratio.

Theocaris *et al.* evaluated the T-criterion on the boundary of the plastic zone as predicted by the Mises yield criterion [3] (figure 3.5). The shape of this boundary can be computed once the stresses around the crack tip are known from e.g. equation (3.3.a) to (3.3.c). In these equations, both the mode I and mode II stress intensity factors and the T-stress can be retained.

At this point, it may be useful to note that the names "T-stress" and "T-criterion" may indicate a closer link than actually exists. The T-stress indicates a constant stress in the region of the crack tip, as used e.g. by Cotterell and Rice [27]. The T-criterion is linked to the distribution of the total strain energy density T and thus addresses a basically different physical quantity.

Returning to the T-criterion, Theocaris et al. stated that the crack would propagate into the direction where the dilatational part T_V of the strain energy density has its maximum along the boundary of the plastic zone. they stated that at this point, the void growth during stable tearing would be maximal since the void growth is controlled by the dilatational part of the energy density. At the plastic boundary defined by the Mises yield criterion, the deformational energy density T_D is constant. They argued that "the T_D component prepares the material around the crack tip for fracture by forming a plastic zone, and the T_V-component provokes crack propagation" by enabling void-growth.

In this study, an attempt will be made to study the predictive value of the T-criterion to the experiments performed on the aluminium specimens. In order to apply this criterion, one requires the yield stress of Al 7075-T6 and Al 2024-T3. Three tensile tests were performed for each material (table 3.10). The yield stress of Al 7075-T6 and Al 2024-T3 was used to determine the shape and size of the Mises yield zone in the T-criterion, taking into account the presence of the T-stress around the crack. The location and magnitude of the maximal dilatational

energy density along the Mises yield boundary was determined. Both the magnitude and the location are presented in table 3.11 and 3.12. Both the magnitude of the dilatational energy density at the failure location and the radius from that point to the crack tip can be used as failure criterion [3,4]. As can be seen in figure 3.11 and 3.12, neither seems to work for the present experiments. For the GLARE-3 specimens, an attempt is not made to apply the T-criterion, although there does not seems to be a theoretical problem for doing so.

3.3 Theoretical validity of the Westergaard equations

Using a geometrically linear theory of elasticity, the Westergaard equation find that the initially sharp crack tip will become elliptical. The amplitude of this ellipse varies linearly with the amplitude of the loading. However, from the very first loading, the crack tip becomes blunt. The basic condition from the linear theory of elasticity is that the shape of the deformed structure is represented by the shape of the undeformed structure. To obtain this, the displacements should remain small and the rotations (or displacement gradients) should remain zero in the limit to zero loading. This last condition is violated in the Westergaard equations: at the crack tip, the rotations are 90° in the linear elastic solution, even in the limit towards zero loading. Thus, the stresses in the crack faces are rotated over 90° and equilibrium is no longer certain. Practically, the crack tip is stretched due to the geometrically non-linearity beside the bending as described in the linear elastic solution.

4 Discussion and conclusions

Looking back at the experiments performed on the three materials and theoretical evaluations associated with them, the failure model of Williams and Ewing [1,2] seems to work best. This does not directly prove the validity of the model. The model of Williams and Ewing has one variable that can be chosen freely, allowing an optimization for the correlation with the experimental results. For the present experiments, this correlation was optimized for the changing failure load for changing crack tilt angles. For Al 7075-T6 and GLARE-3, the failure load of all specimens could quite well be linked to the failure load of the specimen with its crack perpendicular to the loading (figure 3.14). For Al 2024-T3, its performance did not exceed the performance of the nett-section yield criterion (figure 3.14). In stiffened, infinite sheets however, the nett-section yield criterion is difficult to use.

All models seem to predict similar crack propagation directions (see e.g. figure 3.15). The variation in the predicted directions seems smaller than the scatter fund in the present experiments (figure 2.2). In other types of specimens, such as e.g. the compact tension specimen, more variation in propagation direction might be found. In such specimens too, the influence of the fibres in GLARE on the crack propagation might be investigated. For the present specimens, the fibre direction was roughly aligned with the expected failure direction for all kink angles.

The model of Williams and Ewing does not explain the size effects found in residual strength experiments. In front of a crack loaded by a mode I loading only, the T-stress does not have an influence on the hoop stress σ_θ in the model of Williams and Ewing. The T-stress is however known to have an influence on residual strength [19]. The T-criterion of Theocaris *et al.* [3,4] would show the influence of the T-stress on the plastic zone and thus attempt to model the size effect. The T-criterion however, does not seem to work for the present specimens (figure 3.11 and 3.12).

The model of Williams and Ewing was used by Finnie and Saith to model the path stability of cracks [6,7]. Although Williams' and Ewing's failure radius r_c as found for the present tilted cracks, could be used to predict the path stability of mode I cracks, a theoretical problem should be mentioned. From the tilted position, the crack propagates with a kink. A crack with an unstable path will curve from that path. Since both propagation types have a different shape, they may not be governed by the same value of the variable r_c. The variable r_c might be seen as a realistic radius from the crack tip at which the material would fail. Since the Westergaard equations, which form the basis of all elastic failure models, are not valid at the crack tip, this might not be true. The variable r_c might more likely be seen as a fictitious radius showing the balance between the stress intensities and the T-stress in determining the propagation direction and shape. Than, there might exist a different balance for kinking cracks and for cracks with unstable paths.

Concluding, one might say that all the materials presently tested, the failure load increases with increasing crack tilt angle. For Al 7075-T6 and GLARE-3, also the nett-section stress at failure increased. The model of Williams' and Ewing seems to perform best in predicting the variation in failure load, mainly due to the one free variable in it. For Al 2024-T3 the nett section yield criterion did as well as the model of Williams and Ewing. GLARE-3 does not seem to be as sensitive to nett-section yield as AL 2024-T3, nor does it seem to be as brittle as Al 7075-T6.

Acknowledgement

The experiments and calculations were performed in the Structures and Materials Laboratory of the Faculty of Aerospace Engineering in Delft. The GLARE-3 material was supplied by Structural Laminates BV, for which they are thanked.

References

[1] J.G. Williams and P.D. Ewing, Fracture under complex stress - The angled crack problem. *Int. J. Fracture Mech.* **8**, 441-446 (1972).

[2] P.D. Ewing and J.G. Williams, Further observations on the angled crack problem. *Int. J. of Fracture* **10**, 135 (1974).

[3] P.S. Theocaris and N. P. Andrianopolous, The Mises elastic-plastic boundary as the core region in fracture criteria. *Engng Fracture Mech.* **16**, 425-432 (1982).

[4] P.S. Theocaris, G.A. Kardomateas and N.P. Andrianopoulos, Experimental study of the T-criterion in ductile fracture. *Engng Fracture Mech.* **17**, 439-447 (1982).

[5] G. Roebroeks, *Towards GLARE, the development of a fatigue insensitive and damage tolerant aircraft material.* PhD. Thesis, F aculty of Aerospace Engineering, Delft University of Technology, Delft, Netherlands (1992).

[6] I. Finnie and A. Saith, A note on the angled crack problem and the directional stability of cracks. *Int. J. Fracture* **9**, 484-486 (1973).

[7] K.J.J.M. Zaal, *A survey of crack path stability criteria and their application to crack flapping phenomena in stiffened structures.* Report LR-681, Faculty of Aerospace Engineering, Delft University of Technology, Delft, Netherlands (1991).

[8] N. Ohrloff and P. Horst, Feasibility study of the application of GLARE materials in wide body aircraft fuselages. In *Advanced Materials and Structures from Research to Application*, Eds. J. Brandt, H. Hornfeld and M. Neitzel, SAMPE European Chapter (1992).

[9] F. Erdogan and G.C. Sih, On the crack extension in plates under plane loading and transverse shear, *Journal of Basic Engineering, ASME*, **519-527** (1963).

[10] J. Schijve, *Lecture notes on fatigue, static tensile strength and stress corrosion of aircraft materials and structures.* Report LR-360 Faculty of Aerospace Engineering, Delft University of Technology, Delft, Netherlands (1982).

[11] M.M. Ghassem and T.P. Rich, The fracture diagram: a new design tool for stiffened panels. *AIAA Journal* **21**, 1294-1300 (1983).

[12] D.S. Dugdale, Yielding of steel sheets containing slits. *J. Mech. Phys. Solids* **8**, 100-104 (1960).

[13] M.C. Low and D.J. Cartwright, *Fracture diagrams for stiffened aircraft structures: effects of material non-linearity.* In Durability and Damage Tolerance in Aircraft Design, Proceedings of the 13th Symposium of the ICAF 22-24 May, Eds. A. Salvetti and G. Cavallini, 551-583 (1985).

[14] T.P. Rich, M.M. Ghassem and D.J. Cartwright, Fracture diagrams for cracked stiffened panels. *Engng Fracture Mech.* **21**, 1005-1017 (1985).

[15] J.D. Landes, D.E. McCabe and H.A. Ernst, Geometry effects on the R-curve. *Non-Linear Fracture Mechanics: Vol. II - Elastic-Plastic Fracture, ASTM STP 995*, eds. J.D. Landes, A Saxena and J.G. Merkle, ASTM, Philidelphia, 123-143 (1989).

[16] H.M. Westergaard, Bearing pressures and cracks. Journal of Applied Mechanics, A49-53 June (1939).

[17] J.W. Hutchinson, Singular behavior at the end of a tensile crack in a hardening material. *Journal of the Mechanics and Physics of Solids* **16** 13-31 (1986).

[18] J.R.Rice and G.F. Rosengren, Plane strain deformation near crack tip in a power law hardening material. *Journal of the Mechanics and Physics of Solids* **16** 1-12 (1986).

[19] S.G. Larsson and A.J. Carlsson, Influence of non-singular terms and specimen geometry on small-scale yielding at crack tips in elastic plastic plates. *J. Mech. Phys. Solids* 21 263-277 (1973).

[20] R.N.L. Smith, Second order terms and strain energy density for the angled crack problem. *Engng Fracture Mech.* **26** 463-469 (1987).

[21] J. Eftis, D.L.Jones and H. Liebowitz, Load biaxiallity and fracture: synthesis and summary. *Engng Fracture Mech.* **36**, 537-574 (1990).

[22] S.G. Lekhnitskii, *Anisotropic plates*. Translated from the 2nd Russian edition by S.W. Tsai and T. Cheron, Gordon and Breach Science Publishers, New York (1968).

[23] G.C. Sih and E.P. Chen, *Cracks in composite materials*. Martinus Nijhoff, Netherlands (1981).

[24] Th. de Jong, *Mechanica van composiet materialen*. Report LR-431 (In Dutch), Faculty of Aerospace Engineering, Delft University of Technology, Delft, Netherlands (1984).

[25] M. Kosai, A.S. Kobayashi and M. Ramulu, Tear straps in airplane fuselage. *International Workshop on structural integrity of aging airplanes*, Atlanta, 31 March - 2 April (1992).

[26] R.L. Bisplinghoff, J.W. Mar and T.H.H. Pian, *Statics of deformable solids*. Addison-Wesley Publishing Company, Reading, Massachusetts (1965).

[27] B. Cotterell and J.R. Rice, Slightly curved or kinked cracks. *Int. J. Fracture* **16**, 155-169 (1980).

Material property		Al 7075-T6 CLAD	Al 2024-T3 CLAD	GLARE-3 3/2 lay-up, t_{al} = 0.3 mm
t	[mm]	1.6	1.6	1.4
E_x	[MPa]	72400	72400	58200
E_y	[MPa]	72400	72400	58200
G_{xy}	[MPa]	27200	27200	19300
ν_{xy}	-	0.33	0.33	0.288
ν_{yx}	-	0.33	0.33	0.288

Table 2.1: Properties of the materials used in the experiments

Length L	400 mm
Width W	160 mm
Crack length 2a	40 mm
Crack tilt angle α	see table 2.3

Table 2.2: Geometrical properties of the uni-directionally loaded test specimens

Specimen number	Crack tilt angle α
I	0°
II	15°
III	30°
IV	45°
V	60°
VI	75°

Table 2.3: Crack tilt angle for the various specimens

Specimen number	Crack tilt angle α [°]	Failure load Al 7075-T6 specimens P_{fail} [kN]	Failure load Al 2024-T3 specimens P_{fail} [kN]	Failure load GLARE-3 specimens P_{fail} [kN]
I	0°	73.40	69.66	55.24
II	15°	72.17	67.72	55.90
III	30°	72.68	73.20	58.40
IV	45°	78.80	75.36	61.16
V	60°	89.72	81.80	66.44
VI	75°	122.88	88.68	78.80

Table 2.4: Failure load for all specimens

Crack tilt angle α [°]	Failure stress σ_{fail} [MPa]	Nominal failure stress $\frac{\sigma_{fail}}{\sigma_{fail,\,0°}}$	Failure nett stress σ_{nett} [MPa]	Nominal failure nett-stress $\frac{\sigma_{nett}}{\sigma_{nett,\,0°}}$
0°	287	1.00	382	1.00
15°	282	0.98	372	0.97
30°	284	0.99	362	0.95
45°	308	1.07	374	0.98
60°	350	1.22	401	1.05
75°	480	1.67	513	1.34

Table 3.1: Failure stress and nett-section failure stress for the aluminium 7075-T6 specimens

Crack tilt angle α [°]	Failure stress σ_{fail} [MPa]	Nominal failure stress $\frac{\sigma_{fail}}{\sigma_{fail,\,0°}}$	Failure nett stress σ_{nett} [MPa]	Nominal failure nett-stress $\frac{\sigma_{nett}}{\sigma_{nett,\,0°}}$
0°	272	1.00	363	1.00
15°	265	0.97	349	0.96
30°	286	1.05	365	1.01
45°	294	1.08	358	0.99
60°	320	1.17	365	1.01
75°	346	1.27	370	1.02

Table 3.2: Failure stress and nett-section failure stress for the aluminium 2024-T3 specimens

Crack tilt angle α [°]	Failure stress σ_{fail} [MPa]	Nominal failure stress $\frac{\sigma_{fail}}{\sigma_{fail,\,0°}}$	Failure nett stress σ_{nett} [MPa]	Nominal failure nett-stress $\frac{\sigma_{nett}}{\sigma_{nett,\,0°}}$
0°	247	1.00	329	1.00
15°	250	1.01	329	1.00
30°	261	1.06	333	1.01
45°	273	1.11	332	1.01
60°	297	1.20	339	1.03
75°	352	1.43	376	1.14

Table 3.3: Failure stress and nett-section failure stress for the GLARE-3 specimens

Crack tilt angle α [°]	Failure stress $\sigma_{\theta,fail}\sqrt{2\pi r}$ [MPa$\sqrt{mm}$]	Predicted crack propagation angle θ_{pred} [°]	Nominal failure stress $\frac{\sigma_{\theta,\,fail}}{\sigma_{\theta,\,fail,\,0°}}$
0	2273	0	1.00
15	2287	27	1.01
30	2287	43	1.01
45	2182	53	0.96
60	1804	60	0.79
75	1244	66	0.55

Table 3.4: Failure hoop stress in Erdogan's model for the aluminium 7075-T6 specimens

Crack tilt angle α [°]	Failure stress $\sigma_{\theta,fail}\sqrt{2\pi r}$ [MPa$\sqrt{mm}$]	Predicted crack propagation angle θ_{pred} [°]	Nominal failure stress $\frac{\sigma_{\theta,\,fail}}{\sigma_{\theta,\,fail,\,0°}}$
0	2156	0	1.00
15	2149	27	1.00
30	2303	43	1.07
45	2084	53	0.97
60	1647	60	0.76
75	896	66	0.42

Table 3.5: Failure hoop stress in Erdogan's model for the aluminium 2024-T3 specimens

Crack tilt angle α [°]	Failure stress $\sigma_{\theta,fail}\sqrt{2\pi r}$ [MPa$\sqrt{mm}$]	Predicted crack propagation angle θ_{pred} [°]	Nominal failure stress $\frac{\sigma_{\theta,\,fail}}{\sigma_{\theta,\,fail,\,0°}}$
0	1958	0	1.00
15	2031	27	1.04
30	2111	44	1.08
45	1926	53	0.98
60	1505	59	0.77
75	903	65	0.46

Table 3.6: Failure hoop stress in Erdogan's model applied to the average stresses in the laminate, for the GLARE-3 specimens

Crack tilt angle α [°]	Williams' model $r_c = 1.5$			Williams' model $r_c = 1.18$		
	Failure stress		Predicted propagation angle θ_{pred} [°]	Failure stress		Predicted propagation angle θ_{pred} [°]
	Absolute $\sigma_{\theta,fail}$ [MPa]	Nominal $\frac{\sigma_{\theta,\,fail}}{\sigma_{\theta,\,fail,\,0°}}$		Absolute $\sigma_{\theta,fail}$ [MPa]	Nominal $\frac{\sigma_{\theta,\,fail}}{\sigma_{\theta,\,fail,\,0°}}$	
0	741	1.00	0	835	1.00	0
15	716	0.97	15	809	0.97	16
30	691	0.93	33	785	0.94	34
45	711	0.96	53	802	0.96	53
60	731	0.99	69	804	0.96	68
75	791	1.07	80	841	1.01	80

Table 3.7: Failure hoop stress in Williams' model for the aluminium 7075-T6 specimens

Crack tilt angle α [°]	Williams' model $r_c = 1.5$			Williams' model $r_c = 2.95$		
	Failure stress		Predicted propagation angle θ_{pred} [°]	Failure stress		Predicted propagation angle θ_{pred} [°]
	Absolute $\sigma_{\theta,fail}$ [MPa]	Nominal $\frac{\sigma_{\theta,fail}}{\sigma_{\theta,fail,0°}}$		Absolute $\sigma_{\theta,fail}$ [MPa]	Nominal $\frac{\sigma_{\theta,fail}}{\sigma_{\theta,fail,0°}}$	
0	702	1.00	0	502	1.00	0
15	673	0.96	15	477	0.95	13
30	696	0.99	33	486	0.97	30
45	679	0.97	53	485	0.97	53
60	668	0.95	69	512	1.03	72
75	570	0.81	80	491	0.98	82

Table 3.8: Failure hoop stress in Williams' model for the aluminium 2024-T3 specimens

Crack tilt angle α [°]	Williams' model applied to average stresses in laminate, $r_c = 2.01$			Williams' model applied to stresses in aluminium layers only, $r_c = 2.95$		
	Failure stress		Predicted propagation angle θ_{pred} [°]	Failure stress		Predicted propagation angle θ_{pred} [°]
	Absolute $\sigma_{\theta,fail}$ [MPa]	Nominal $\frac{\sigma_{\theta,fail}}{\sigma_{\theta,fail,0°}}$		Absolute $\sigma_{\theta,fail}$ [MPa]	Nominal $\frac{\sigma_{\theta,fail}}{\sigma_{\theta,fail,0°}}$	
0	51	1.00	0	587	1.00	0
15	546	0.99	14	597	1.02	13
30	543	0.98	31	587	1.00	28
45	542	0.98	53	580	0.99	54
60	555	1.01	70	652	1.11	72
75	547	0.99	82	667	1.14	81

Table 3.9: Failure hoop stress in Williams' model applied to the average stresses in the laminate and to the stresses in the aluminium layers, for the GLARE-3 specimens

Specimen number	Al 7075-T6 t = 1.6 mm		Al 2024-T3 t = 1.6 mm		GLARE-3 t = 1.4 mm	
	Yield stress $\sigma_{0.2}$	Ultimate stress σ_{ult}	Yield stress $\sigma_{0.2}$	Ultimate stress σ_{ult}	Yield stress $\sigma_{0.2}$	Ultimate stress σ_{ult}
I	517	561	394	477	316	713
II	515	565	393	472	323	721
III	513	563	392	473	319	734
Average:	515	563	393	474	319	722

Table 3.10: Yield and ultimate stress for the materials used in the experiments

Crack tilt angle α [°]	Distortional strain energy density at failure location		Plastic radius at failure location		Predicted propagation angle θ_{pred}[°]
	Absolute $T_{V,fail}$ [Nmm/mm^3]	Nominal $\frac{T_{V,fail}}{T_{V,fail,0°}}$	Absolute $r_{pl,fail}$ [mm]	Nominal $\frac{r_{pl,fail}}{r_{pl,fail,0°}}$	
0	0.637	1.00	3.10	1.00	0
15	0.666	1.05	2.85	0.92	19
30	0.687	1.08	2.46	0.79	39
45	0.635	1.00	2.18	0.70	60
60	0.495	0.78	1.62	0.52	77
75	0.289	0.45	0.91	0.29	93
	$\sigma_{0.2}$ = 483 MPa				

Table 3.11: The failure model of Theocaris et al. for the aluminium 7075-T6 specimens

Crack tilt angle α [°]	Distortional strain energy density at failure location		Plastic radius at failure location		Predicted propagation angle θ_{pred}[°]
	Absolute $T_{V,fail}$ [Nmm/mm^3]	Nominal $\frac{T_{V,fail}}{T_{V,fail,0°}}$	Absolute $r_{pl,fail}$ [mm]	Nominal $\frac{r_{pl,fail}}{r_{pl,fail,0°}}$	
0	0.310	1.00	4.79	1.00	0
15	0.347	1.12	4.34	0.91	18
30	0.380	1.23	4.30	0.90	38
45	0.370	1.19	3.42	0.71	60
60	0.281	0.91	2.36	0.49	78
75	0.177	0.57	0.80	0.17	92
	$\sigma_{0.2}$ = 393 MPa				

Table 3.12: The failure model of Theocaris et al. for the aluminium 2024-T3 specimens

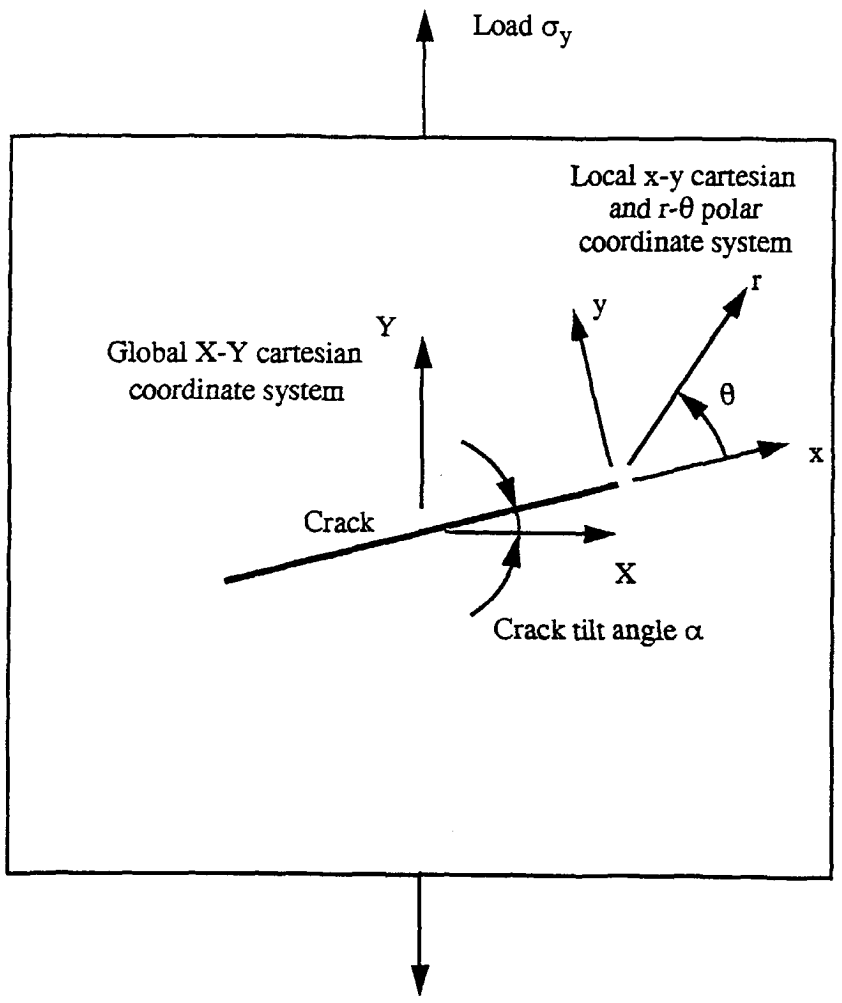

a: global and local coordinate systems around the angled crack

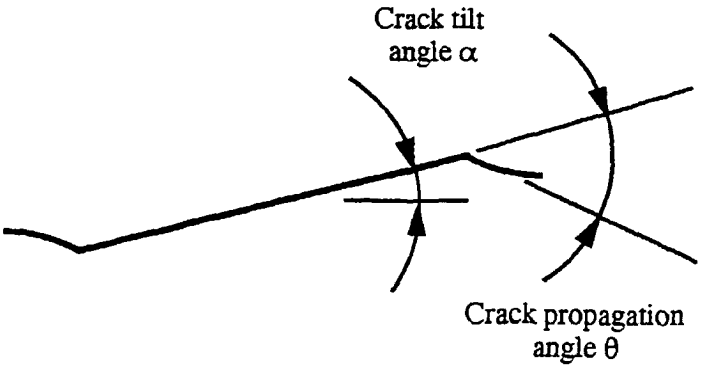

b: shape of expected crack propagation

Figure 1.1: The angled crack in a uni-directionally loaded plate

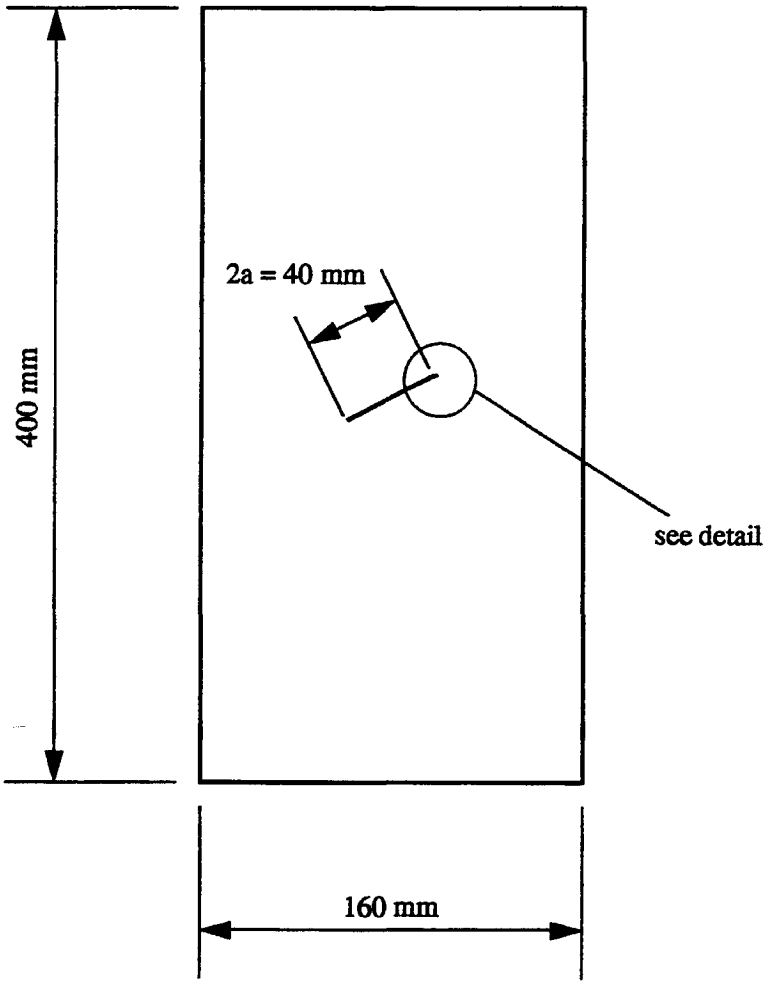

a: Test specimen

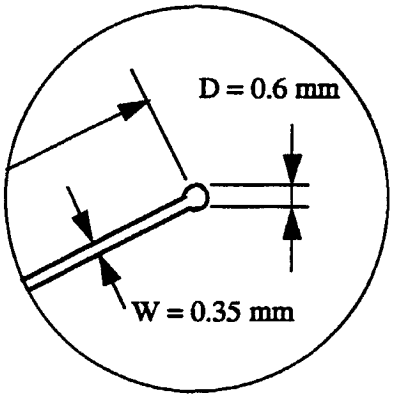

b: Detail of crack tip

Figure 2.1: Uni-directionally loaded specimen, with centrally, angled crack

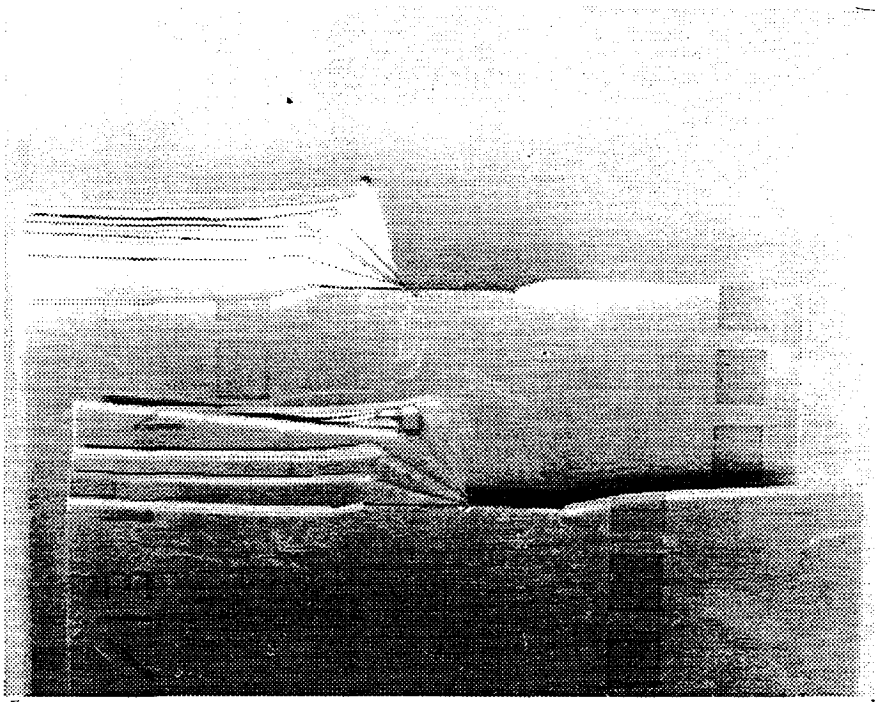

Figure 2.2: Crack propagation directions from the angled cracks in the Al 7075-T6 specimens

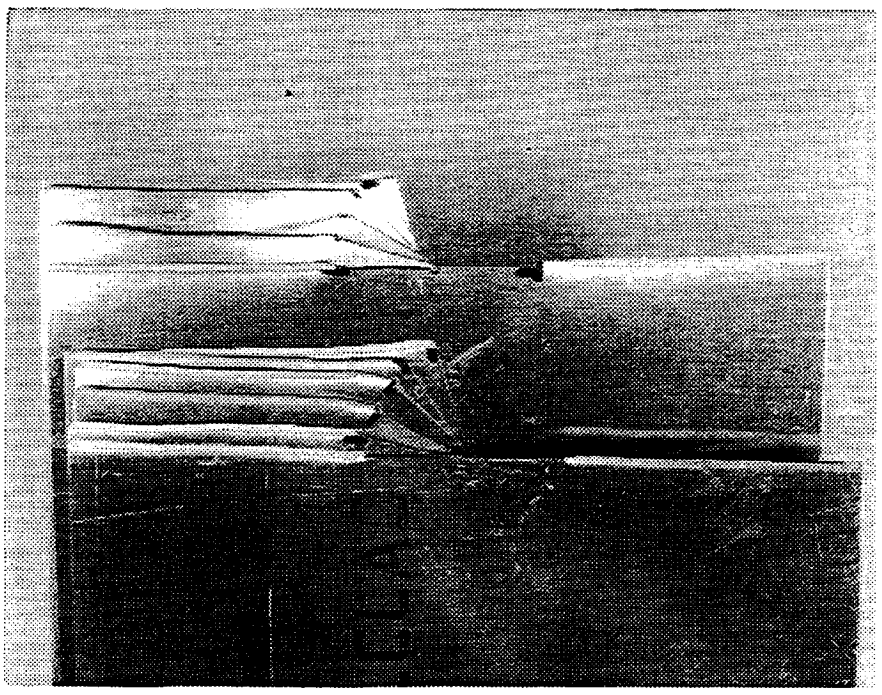

Figure 2.3: Crack propagation directions from the angled cracks in the Al 2024-T3 specimens

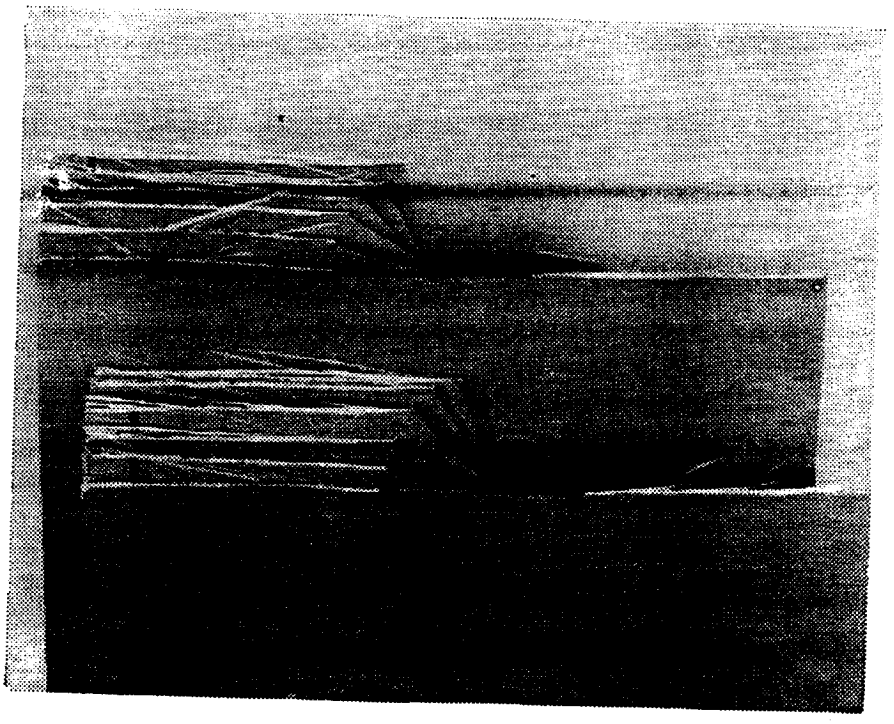

Figure 2.4: Crack propagation directions from the angled cracks in the GLARE-3 specimens

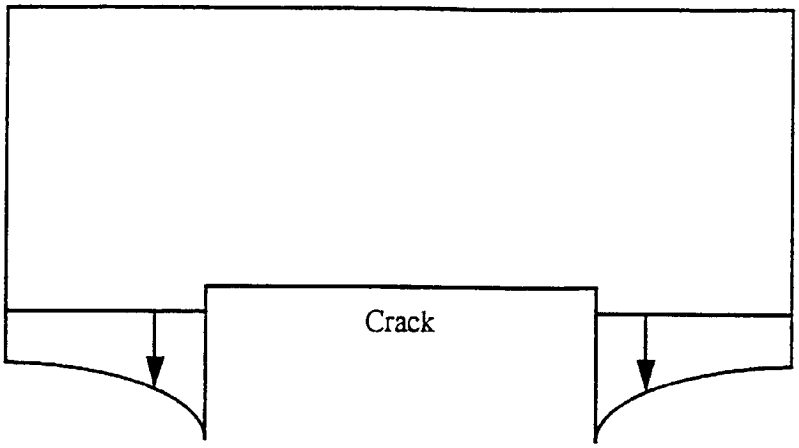

Strain distribution $\varepsilon(x)$

a: Strain distribution along the nett-section in a centre cracked plate

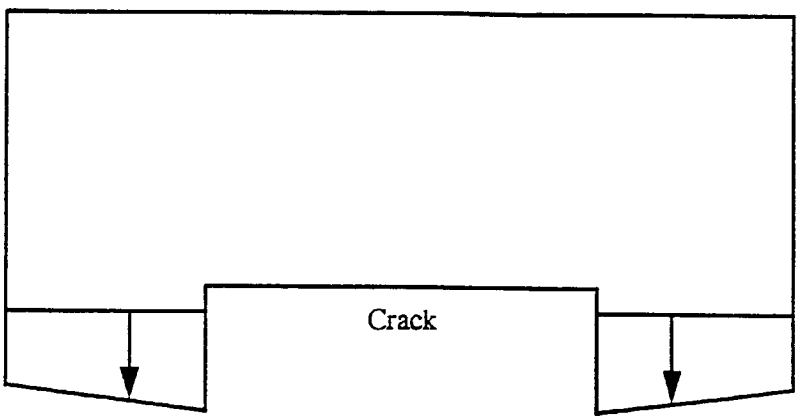

Stress distribution $\sigma(x)$

b: Resulting stress distribution for non-hardening alloys

Figure 3.1: Nett-section yield failure model

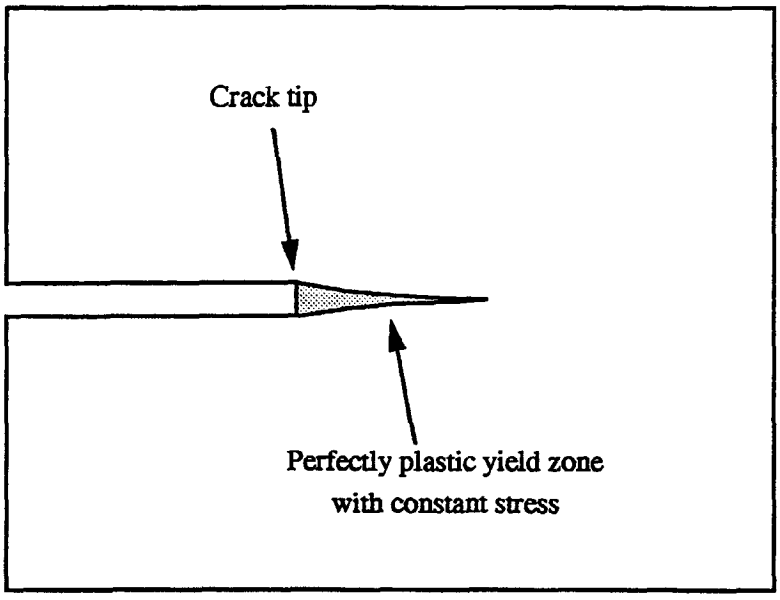

Figure 3.2: Dugdale model with original material in perfectly plastic state bridging the crack near the tip

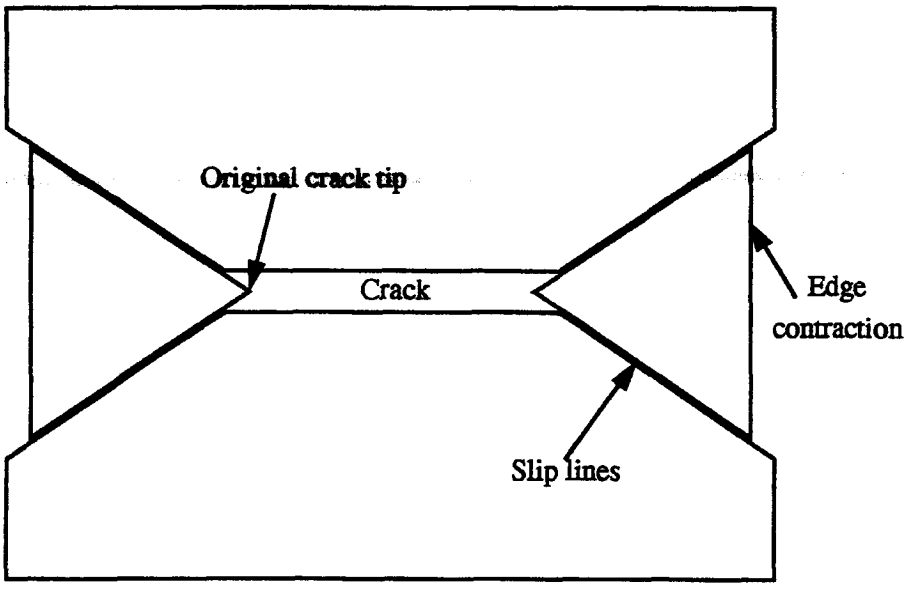

Figure 3.3: Failure mode of centre cracked plate in limit analysis, using slip lines on the plate surface

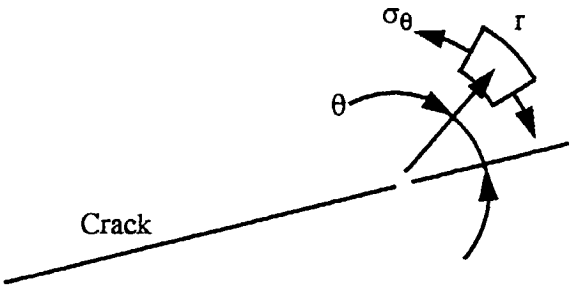

Figure 3.4: Hoop stress around a crack tip in the maximal hoop stress criterion

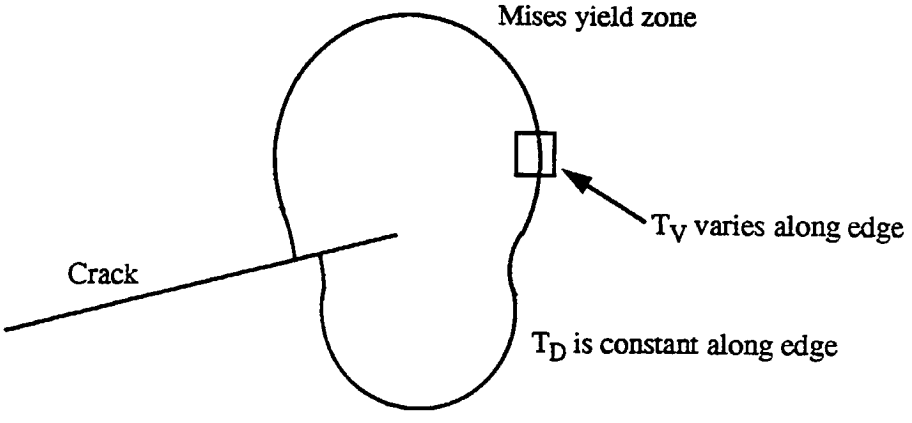

Figure 3.5: Strain energy density along the edge of the Mises yield zone

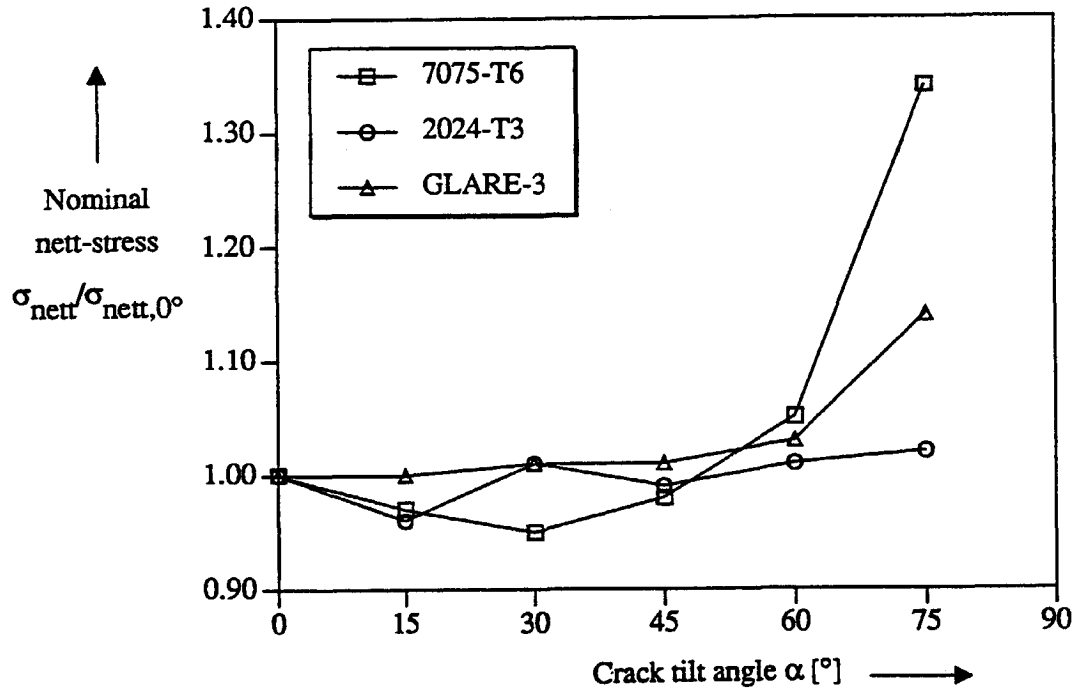

Figure 3.6: Nominal nett-section failure stress

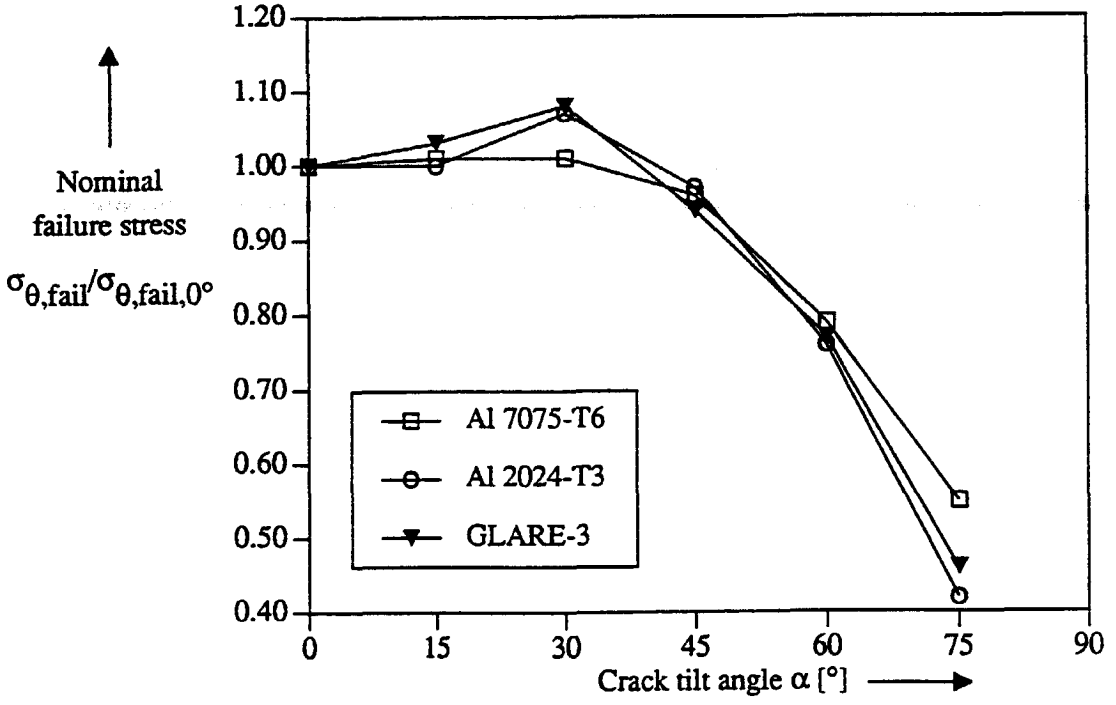

Figure 3.7: Nominal failure hoop stress using Erdogan's model

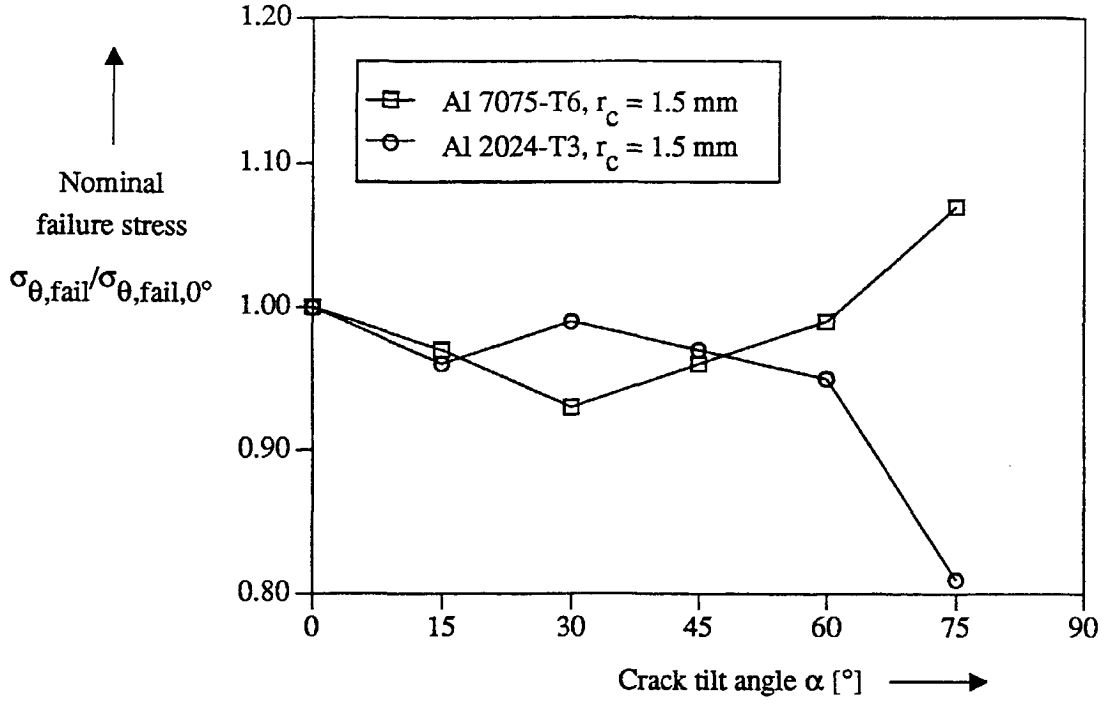

Figure 3.8: Nominal failure hoop stress using Williams' model and Kobayashi's value for rc

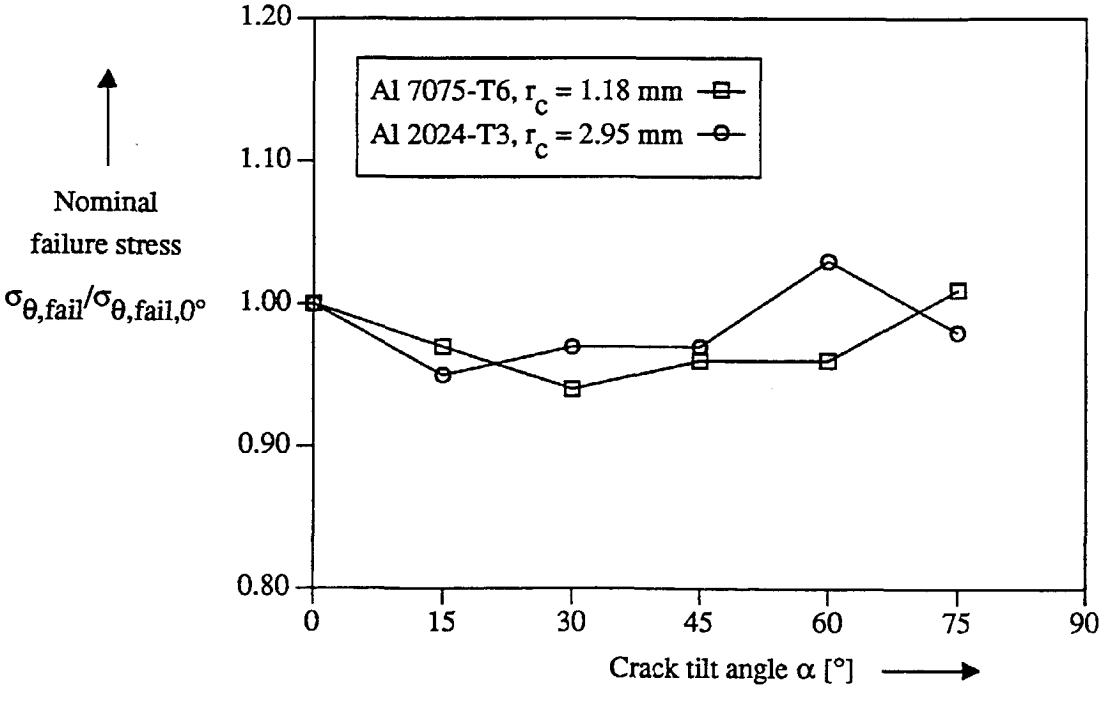

Figure 3.9: Nominal failure hoop stress using Williams' model and an optimized value for rc

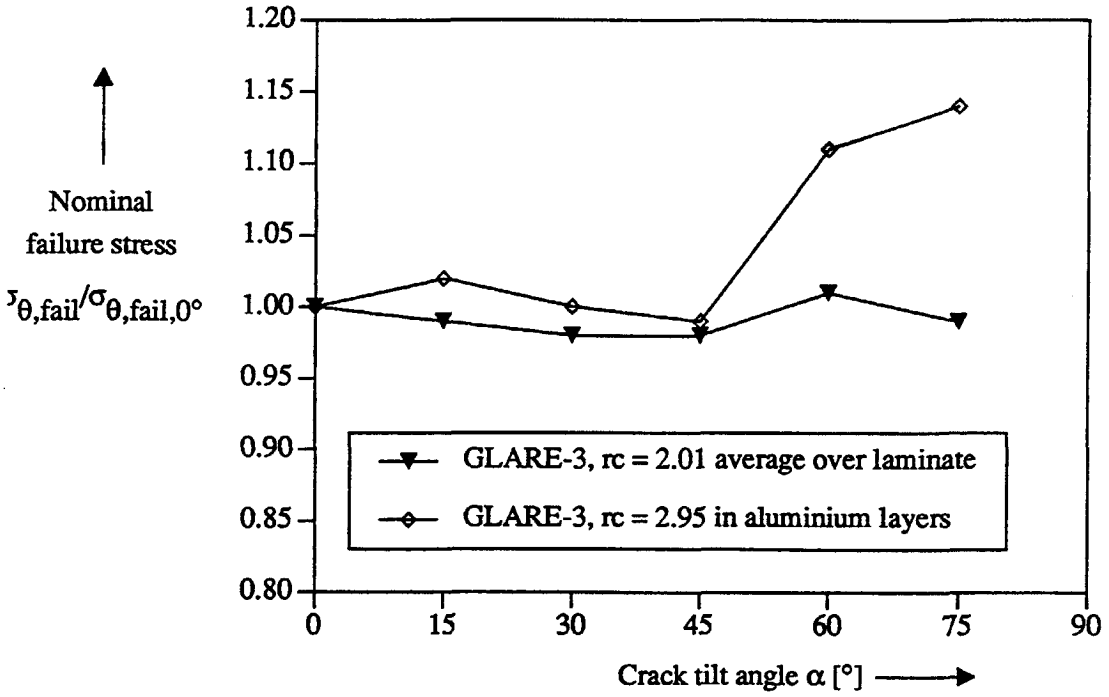

Table 3.10: Nominal failure hoop stress in Williams' model applied to the average stresses in the laminate and to the stresses in the aluminium layers, for the GLARE-3 specimens

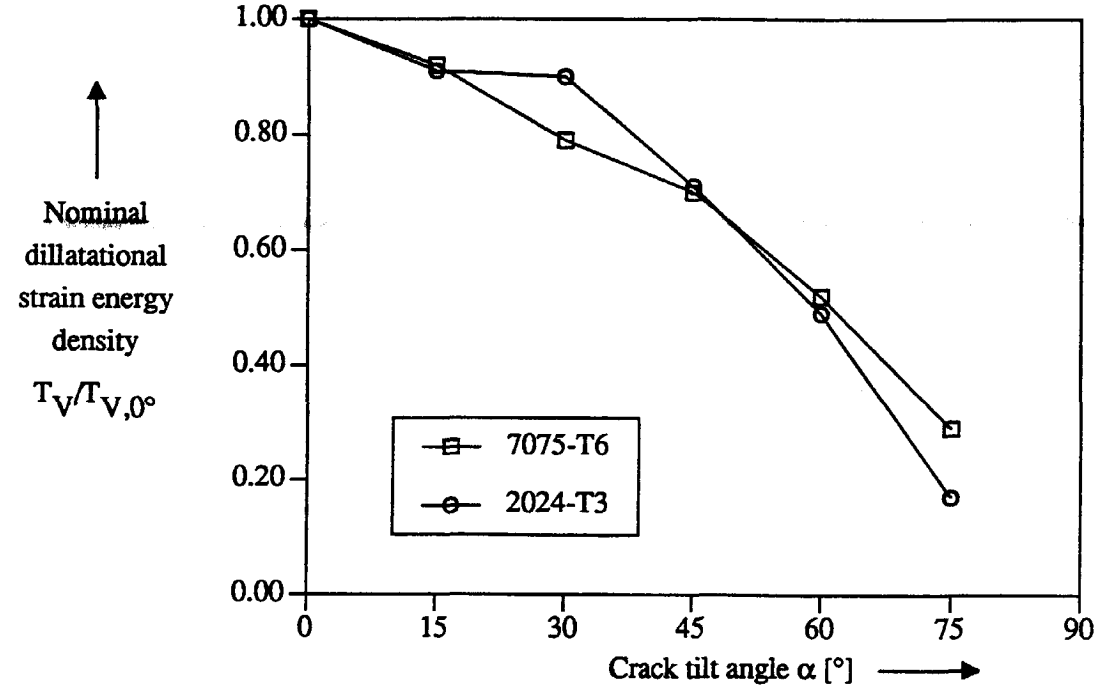

Figure 3.11: Nominal failure dilatational energy density using the model of Theocaris et al.

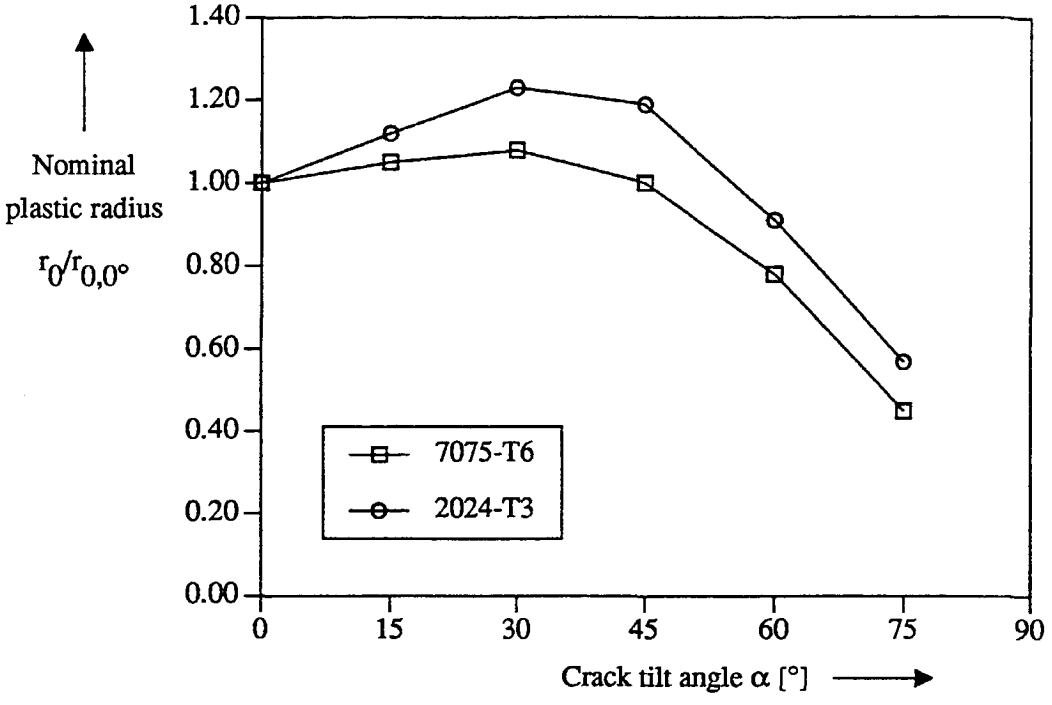

Figure 3.12: Nominal plastic radius at location of maximal dilatational energy density using the model of Theocaris et al.

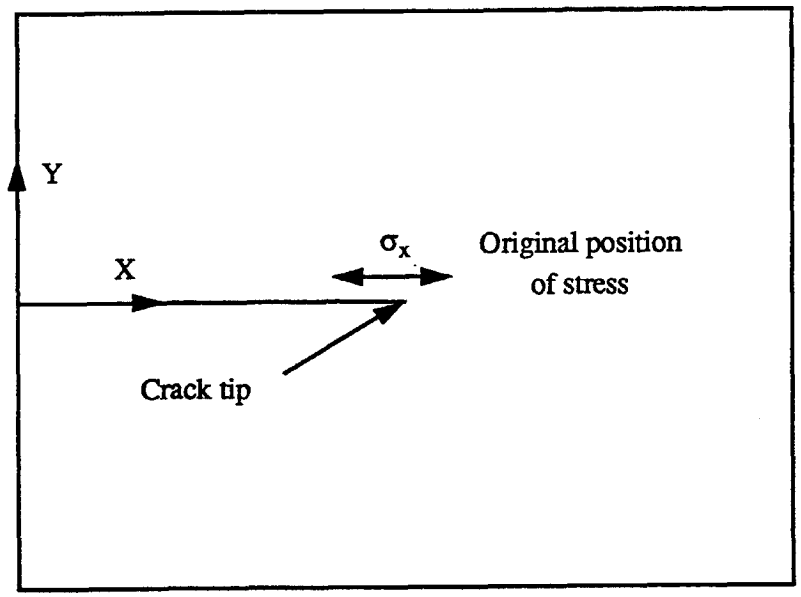

a: undeformed crack tip

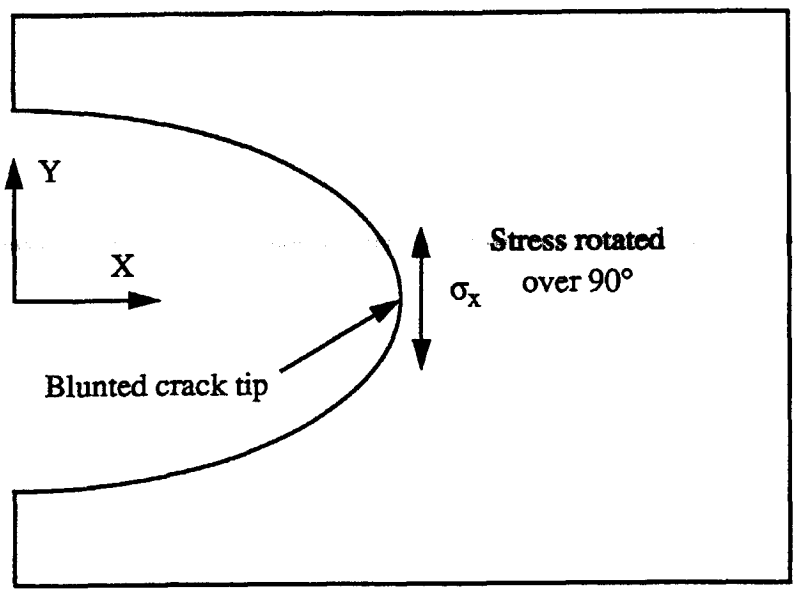

b: crack tip in deformed state, with geometrical non-linearity at crack tip

Figure 3.13: Geometrical non-linearity in the Westergaard equations describing the deformations around a crack tip

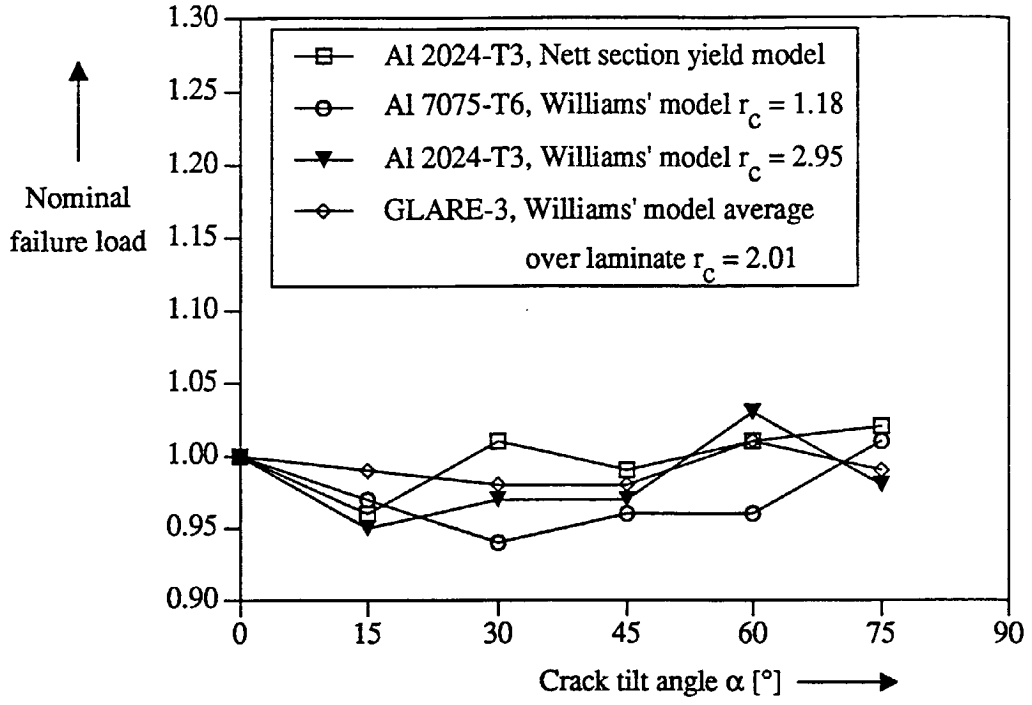

Figure 3.14: A summary of the predictions of Williams' and Ewing's model and the nett-section yield criterion

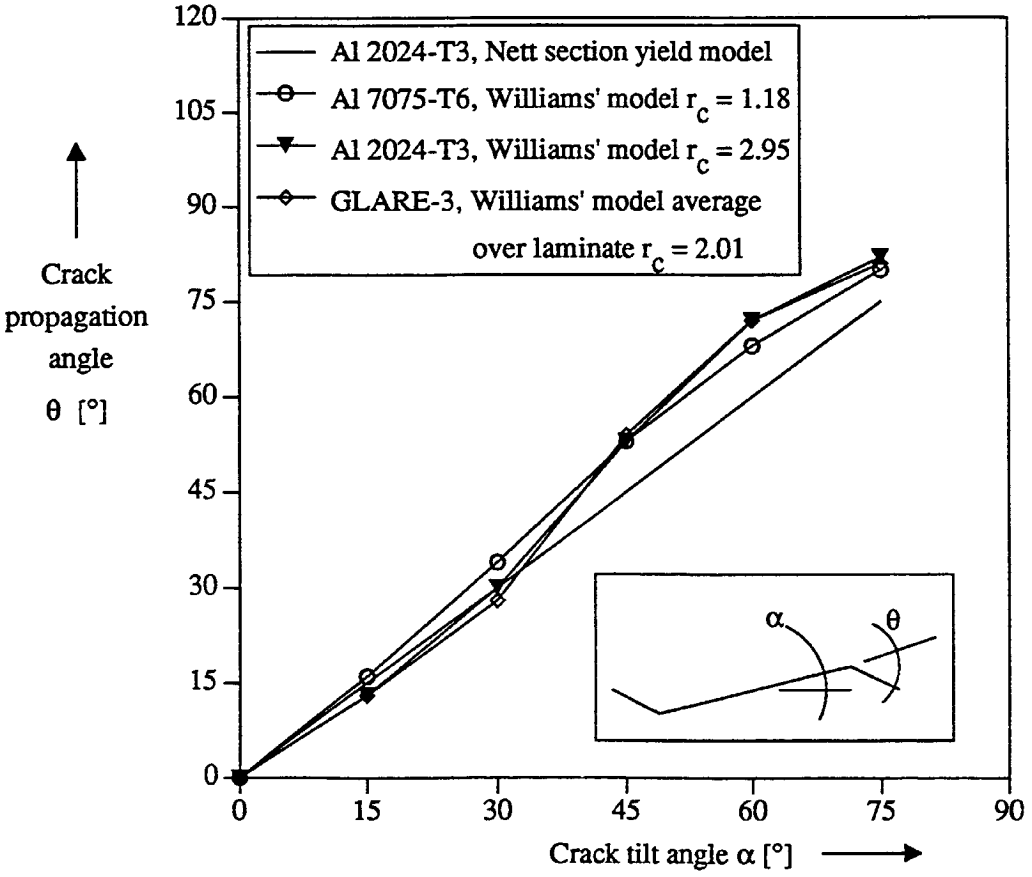

Figure 3.15: Crack propagation directions predicted by the failure model of Williams' and Ewing's model and the nett-section yield criterion

Appendix A: Stress intensities and T-stress in anisotropic plates

In a uni-directionally loaded plate with an angled crack, the crack tip is loaded both in a mode I and in mode II type of deformation (figure a.1.a). Redefining the load on the crack in the local crack coordinate axis, one might split the problem into three parts (figure a.1.b to a.1.d). The first part consists of an uncracked plate loaded in tension and shear (figure a.1.b). The second and third part consist of cracked plates loaded at their crack faces by constant pressure and shear loads p and q (figure a.1.c and a.1.d). The loads at the crack faces can be expressed in the original load σ on the uni-directionally loaded plate with the angled crack, and the tilt angle α. First, the stresses at the crack location in the uncracked plate can be evaluated:

$$\sigma_x = \sigma \sin^2\alpha$$

$$\sigma_y = \sigma \cos^2\alpha$$

$$\tau_{xy} = \sigma \sin\alpha \cos\alpha$$

The stresses σ_y and τ_{xy} have to be eliminated by respectively p and q:

$$p = \sigma_y = \sigma \cos^2\alpha$$

$$q = \tau_{xy} = \sigma \sin\alpha \cos\alpha$$

For these two problems solutions are known [1] and the stress intensities at the crack tip have been derived [2]. For the problem of the crack whose faces are loaded by a constant pressure p, the solution is given as [1]:

$$\phi_1 = \frac{s_2 p\, a}{2(s_1 - s_2)} \frac{1}{\zeta_1}$$

$$\phi_2 = \frac{s_1 p\, a}{2(s_2 - s_1)} \frac{1}{\zeta_2}$$

where:

$$\zeta_1 = \frac{z_1 + \sqrt{z_1^2 - a^2}}{a}$$

$$\zeta_2 = \frac{z_2 + \sqrt{z_2^2 - a^2}}{a}$$

The stresses can be derived with the following equations:

$$\sigma_x = 2\mathrm{Re}\left[s_1^2 \phi'_1(z_1) + s_2^2 \phi'_2(z_2)\right]$$

$$\sigma_y = 2\mathrm{Re}\left[\phi'_1(z_1) + \phi'_2(z_2)\right]$$

$$\tau_{xy} = -2\mathrm{Re}\left[s_1 \phi'_1(z_1) + s_2 \phi'_2(z_2)\right]$$

In order to derive the stress distribution, one requires the derivative of the functions ϕ_1 and ϕ_2 with respect to z_1 and z_2 and thus the derivative of ζ_1 and ζ_2 with respect to z_1 and z_2:

$$\frac{d}{dz_1}\left(\frac{1}{\zeta_1}\right) = \frac{d}{dz_1}\left(\frac{a\left(z_1-\sqrt{z_1^2-a^2}\right)}{z_1^2-\left(z_1^2-a^2\right)}\right) = \frac{d}{dz_1}\left(\frac{z_1-\sqrt{z_1^2-a^2}}{a}\right) = \frac{1}{a}\left(1-\frac{z_1}{\sqrt{z_1^2-a^2}}\right)$$

To derive the stress distribution close to the crack tip, one may take the limit of this derivative towards the crack tip:

$$\lim_{z_1\to a}\left(\frac{1}{a}\left(1-\frac{z_1}{\sqrt{z_1^2-a^2}}\right)\right) = \left(\frac{1}{a}\left(1-\frac{a}{\sqrt{z_1+a}\sqrt{z_1-a}}\right) = \frac{1}{a}\left(1-\frac{a}{\sqrt{2a}\sqrt{r\left(\cos\theta+s_1\sin\theta\right)}}\right)\right)$$

$$= \frac{1}{a}\left(1-\frac{\sqrt{\pi a}}{\sqrt{2\pi r}}\frac{1}{\sqrt{\psi_1}}\right)$$

where:

$$\psi_1 = \cos\theta+s_1\sin\theta$$

Similarly:

$$\frac{d}{dz_2}\left(\frac{1}{\zeta_2}\right) = \frac{1}{a}\left(1-\frac{\sqrt{\pi a}}{\sqrt{2\pi r}}\frac{1}{\sqrt{\psi_2}}\right)$$

where:

$$\psi_2 = \cos\theta+s_2\sin\theta$$

Now, in the limit towards the crack tip all non-vanishing stresses are found to be:

$$\sigma_x = 2\mathrm{Re}\left[\frac{s_1^2 s_2}{2\left(s_1-s_2\right)}p\,a\frac{1}{a}\left(1-\frac{\sqrt{\pi a}}{\sqrt{2\pi r}}\frac{1}{\sqrt{\psi_1}}\right)+\frac{s_2^2 s_1}{2\left(s_2-s_1\right)}p\,a\frac{1}{a}\left(1-\frac{\sqrt{\pi a}}{\sqrt{2\pi r}}\frac{1}{\sqrt{\psi_2}}\right)\right]$$

$$= \mathrm{Re}\left[s_1 s_2 p-\frac{s_1 s_2}{s_1-s_2}\frac{p\sqrt{\pi a}}{\sqrt{2\pi r}}\left(\frac{s_1}{\sqrt{\psi_1}}-\frac{s_2}{\sqrt{\psi_2}}\right)\right] = p\,\mathrm{Re}\left[s_1 s_2\right]-\frac{K_I}{\sqrt{2\pi r}}\mathrm{Re}\left[\frac{s_1 s_2}{s_1-s_2}\left(\frac{s_1}{\sqrt{\psi_1}}-\frac{s_2}{\sqrt{\psi_2}}\right)\right]$$

$$\sigma_y = 2\mathrm{Re}\left[\frac{s_2}{2\left(s_1-s_2\right)}p\,a\frac{1}{a}\left(1-\frac{\sqrt{\pi a}}{\sqrt{2\pi r}}\frac{1}{\sqrt{\psi_1}}\right)+\frac{s_1}{2\left(s_2-s_1\right)}p\,a\frac{1}{a}\left(1-\frac{\sqrt{\pi a}}{\sqrt{2\pi r}}\frac{1}{\sqrt{\psi_2}}\right)\right]$$

$$= \mathrm{Re}\left[-p-\frac{1}{s_1-s_2}\frac{p\sqrt{\pi a}}{\sqrt{2\pi r}}\left(\frac{1}{\sqrt{\psi_1}}-\frac{1}{\sqrt{\psi_2}}\right)\right] = -p-\frac{K_I}{\sqrt{2\pi r}}\mathrm{Re}\left[\frac{1}{s_1-s_2}\left(\frac{s_2}{\sqrt{\psi_1}}-\frac{s_1}{\sqrt{\psi_2}}\right)\right]$$

$$\tau_{xy} = -2\mathrm{Re}\left[\frac{s_1 s_2}{2\left(s_1-s_2\right)}p\,a\frac{1}{a}\left(1-\frac{\sqrt{\pi a}}{\sqrt{2\pi r}}\frac{1}{\sqrt{\psi_1}}\right)+\frac{s_2 s_1}{2\left(s_2-s_1\right)}p\,a\frac{1}{a}\left(1-\frac{\sqrt{\pi a}}{\sqrt{2\pi r}}\frac{1}{\sqrt{\psi_2}}\right)\right]$$

$$= \mathrm{Re}\left[\frac{s_1 s_2}{s_1 - s_2}\frac{p\sqrt{\pi a}}{\sqrt{2\pi r}}\left(\frac{1}{\sqrt{\psi_1}} - \frac{1}{\sqrt{\psi_2}}\right)\right] = \frac{K_I}{\sqrt{2\pi r}}\mathrm{Re}\left[\frac{s_1 s_2}{s_1 - s_2}\left(\frac{1}{\sqrt{\psi_1}} - \frac{1}{\sqrt{\psi_2}}\right)\right]$$

For the second problem - the cracked plate loaded by a shear load at the crack faces - the solution is given as:

$$\phi_1 = \frac{q\,a}{2(s_1 - s_2)}\frac{1}{\zeta_1}$$

$$\phi_2 = \frac{q\,a}{2(s_2 - s_1)}\frac{1}{\zeta_2}$$

Now, the stresses in the limit towards the crack tip are found to be:

$$\sigma_x = 2\mathrm{Re}\left[\frac{s_1^2}{2(s_1 - s_2)} q\,a\frac{1}{a}\left(1 - \frac{\sqrt{\pi a}}{\sqrt{2\pi r}}\frac{1}{\sqrt{\psi_1}}\right) + \frac{s_2^2}{2(s_2 - s_1)} q\,a\frac{1}{a}\left(1 - \frac{\sqrt{\pi a}}{\sqrt{2\pi r}}\frac{1}{\sqrt{\psi_2}}\right)\right]$$

$$= \mathrm{Re}\left[(s_1 + s_2)q - \frac{1}{s_1 - s_2}\frac{q\sqrt{\pi a}}{\sqrt{2\pi r}}\left(\frac{s_1^2}{\sqrt{\psi_1}} - \frac{s_2^2}{\sqrt{\psi_2}}\right)\right] = q\mathrm{Re}[s_1 + s_2] - \frac{K_{II}}{\sqrt{2\pi r}}\mathrm{Re}\left[\frac{1}{s_1 - s_2}\left(\frac{s_1^2}{\sqrt{\psi_1}} - \frac{s_2^2}{\sqrt{\psi_2}}\right)\right]$$

$$\sigma_y = 2\mathrm{Re}\left[\frac{1}{2(s_1 - s_2)} q\,a\frac{1}{a}\left(1 - \frac{\sqrt{\pi a}}{\sqrt{2\pi r}}\frac{1}{\sqrt{\psi_1}}\right) + \frac{1}{2(s_2 - s_1)} q\,a\frac{1}{a}\left(1 - \frac{\sqrt{\pi a}}{\sqrt{2\pi r}}\frac{1}{\sqrt{\psi_2}}\right)\right]$$

$$= \mathrm{Re}\left[-\frac{1}{s_1 - s_2}\frac{q\sqrt{\pi a}}{\sqrt{2\pi r}}\left(\frac{1}{\sqrt{\psi_1}} - \frac{1}{\sqrt{\psi_2}}\right)\right] = -\frac{K_{II}}{\sqrt{2\pi r}}\mathrm{Re}\left[\frac{1}{s_1 - s_2}\left(\frac{1}{\sqrt{\psi_1}} - \frac{1}{\sqrt{\psi_2}}\right)\right]$$

$$\tau_{xy} = -2\mathrm{Re}\left[\frac{s_1}{2(s_1 - s_2)} q\,a\frac{1}{a}\left(1 - \frac{\sqrt{\pi a}}{\sqrt{2\pi r}}\frac{1}{\sqrt{\psi_1}}\right) + \frac{s_2}{2(s_2 - s_1)} q\,a\frac{1}{a}\left(1 - \frac{\sqrt{\pi a}}{\sqrt{2\pi r}}\frac{1}{\sqrt{\psi_2}}\right)\right]$$

$$= \mathrm{Re}\left[-q + \frac{1}{s_1 - s_2}\frac{q\sqrt{\pi a}}{\sqrt{2\pi r}}\left(\frac{1}{\sqrt{\psi_1}} - \frac{1}{\sqrt{\psi_2}}\right)\right] = -q + \frac{K_{II}}{\sqrt{2\pi r}}\mathrm{Re}\left[\frac{1}{s_1 - s_2}\left(\frac{s_1}{\sqrt{\psi_1}} - \frac{s_2}{\sqrt{\psi_2}}\right)\right]$$

In the definition of the stress distribution, the stress intensity factors K_I and K_{II} have been defined as:

$$K_I = p\sqrt{\pi a} = \sigma\cos^2\alpha\sqrt{\pi a}$$

$$K_{II} = q\sqrt{\pi a} = \sigma\sin\alpha\cos\alpha\sqrt{\pi a}$$

The stress intensity factors are equal to the stress intensity factors in the corresponding isotropic solutions. It should however be stressed that the stress distribution solutions in anisotropic materials differ basically from the distributions in isotropic solutions. A similarity approach between cracks in isotropic and anisotropic materials can therefore not be used. Further, a similarity approach between different anisotropic solutions can from an elasticity stand point only be justified if the materials have identical material constants s_1 and s_2.

In anisotropic materials, the mode II crack deformation contributes to the T-stress:

$$T = \sigma\sin^2\alpha + pRe[s_1 s_2] + qRe[s_1 + s_2] = \sigma(\sin^2\alpha + \cos^2\alpha Re[s_1 s_2] + \sin\alpha\cos\alpha Re[s_1 + s_2])$$

This contribution disappears for isotropic materials:

$$T = \sigma(\sin^2\alpha + \cos^2\alpha Re[i^2] + \sin\alpha\cos\alpha Re[i + i]) = \sigma(\sin^2\alpha - \cos^2\alpha) = -\sigma\cos 2\alpha$$

[1] S.G. Lekhnitskii, *Anisotropic plates*. Translated from the 2nd Russian edition by S.W. Tsai and T. Cheron, Gordon and Breach Science Publishers, New York (1968).

[2] Th. de Jong, *Mechanica van composiet materialen*. Report LR-431 (In Dutch), Faculty of Aerospace Engineering, Delft University of Technology, Delft, Netherlands (1984).

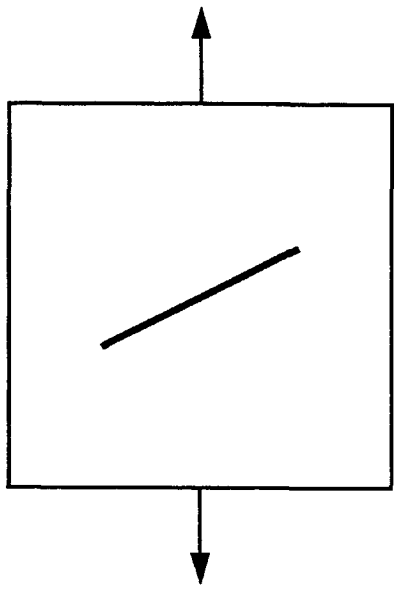

a: angled crack

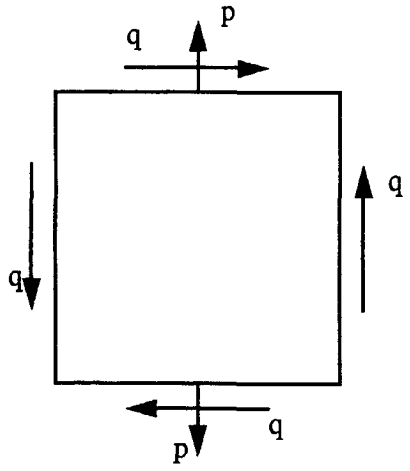

a: uncracked plate loaded in tension and shear

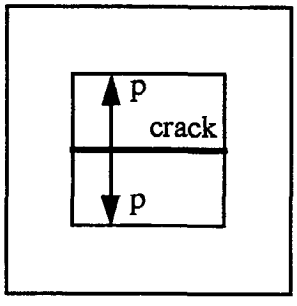

c: pressure load at crack faces

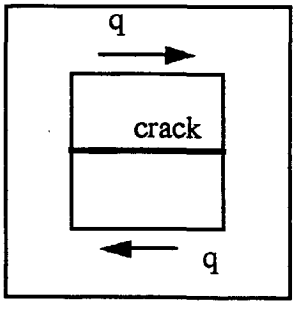

d: shear load at crack faces

Figure a.1: Three way split of uni-directionally loaded plate with angled crack

Appendix B: Stress distribution in laminates

In a laminate, the strains are equal in all layers. They can be expressed in terms of the average laminate stresses and average laminate flexibilities [1]:

$$\begin{bmatrix} \varepsilon_x \\ \varepsilon_y \\ \gamma_{xy} \end{bmatrix}_{lam} = \begin{bmatrix} \frac{1}{E_x} & \frac{-\nu_{yx}}{E_y} & \\ \frac{-\nu_{xy}}{E_x} & \frac{1}{E_y} & \\ & & \frac{1}{G_{xy}} \end{bmatrix}_{lam} \begin{bmatrix} \sigma_x \\ \sigma_y \\ \tau_{xy} \end{bmatrix}_{lam}$$

The stresses in each layer can be computed from these general strains by using he stifness of the individual layers. If e.g. one would require the stresses in an alumnium layer layer, which behaves isotropicaly under the general laminate strains, one would find:

$$\begin{bmatrix} \sigma_x \\ \sigma_y \\ \tau_{xy} \end{bmatrix}_{al} = \begin{bmatrix} \frac{E}{1-\nu^2} & \frac{\nu E}{1-\nu^2} & \\ \frac{E}{1-\nu^2} & \frac{E}{1-\nu^2} & \\ & & G \end{bmatrix}_{al} \begin{bmatrix} \varepsilon_x \\ \varepsilon_y \\ \gamma_{xy} \end{bmatrix}_{lam}$$

Combining these equations, one can link the tensile and shear stresses in the individual alumnium layers to the average stresses in the laminate:

$$\begin{bmatrix} \sigma_x \\ \sigma_y \end{bmatrix}_{al} = \frac{E}{1-\nu^2} \begin{bmatrix} \frac{1-\nu\nu_{xy}}{E_x} & \frac{\nu-\nu_{yx}}{E_y} \\ \frac{\nu-\nu_{yx}}{E_x} & \frac{1-\nu\nu_{xy}}{E_y} \end{bmatrix} \begin{bmatrix} \sigma_x \\ \sigma_y \end{bmatrix}_{lam}$$

$$\begin{bmatrix} \tau_{xy} \end{bmatrix}_{al} = \begin{bmatrix} \frac{G}{G_{xy}} \end{bmatrix} \begin{bmatrix} \tau_{xy} \end{bmatrix}_{lam}$$

[1] Th. de Jong, *Mechanica van composiet materialen.* Report LR-431 (In Dutch), Faculty of Aerospace Engineering, Delft University of Technology, Delft, Netherlands (1984).

Appendix C: Fortran source codes

Source code used to evaluate the hoop stresses σ_θ around a crack tip in an isotropic plate

```
      program isotheta
ccccccccccccccccccccccccccccccccccccccccccccccccccccccccccccccccccccc
c
c     Program to determine the propagation angle of a crack under
c     mixed mode I and II loading
c
ccccccccccccccccccccccccccccccccccccccccccccccccccccccccccccccccccccc
c
c     Variabels used to open the files
c
c-----------------------------------------------------------------------c
c
      integer           nmax
      parameter         (nmax=12)
c
      integer           ipinpf,ipoutf,ipecho
      integer           iflag
      integer           ynscrn,ynecho
      character*20      mfile,ifile,efile
      character*4       letter
      parameter         (ipoutf=8,ipecho=9)
c
c-----------------------------------------------------------------------c
c
c     Variabels used to open the plot window
c
c-----------------------------------------------------------------------c
c
      double precision sigma,pi,a,beta,theta,E,nu
      double precision KI,KII,T,fxi,fyi,fxyi,fxii,fyii,fxyii
      double precision KINOR,KIINOR,fact
      double precision sigmax,sigmay,tauxy,sigmat,themax,rc
      double precision betas,betae,betai,sitmax(nmax),stddev
c
      integer           i,Tyn,j,k
c
      data pi           / 3.141592654 /
c
c-----------------------------------------------------------------------c
c
c     Input from screen or file
c
c-----------------------------------------------------------------------c
c
      write(6,*) 'Input from the screen or from a file (s/f)?'
      read(5,*) letter
c
      if (letter.eq.'f') then
c
         ipinpf = 7
         ynscrn = 0
         ynecho   = 0
c
14       continue
c
         write(6,*) 'Type the input-full file naam:'
         read(5,*) ifile
c
         open(ipinpf,file=ifile,status='old',iostat=iflag)
c
         if (iflag.ne.0) then
c
            write(6,*) 'The file ',ifile,'doesn't exists.'
```

```
            goto 14
c
         endif
c
      else
c
         ipinpf = 5
         ynscrn = 1
         ynecho   = 0
c
         write(6,*) 'Do you want an echo-file of the input (y/n)?'
         read(5,*) letter
c
         if (letter.eq.'y') then
c
            ynecho = 1
c
15          continue
c
            write(6,*) 'Type the full echo-file naam:'
            read(5,*) efile
c
            open(ipecho,file=efile,status='new',iostat=iflag)
c
            if (iflag.ne.0) then
c
               write(6,*) 'The file ',efile,'already exists.'
               goto 15
c
            endif
c
         endif
c
      endif
c
c-----------------------------------------------------------------------c
c
c     Output to outf file
c
c-----------------------------------------------------------------------c
c
16    continue
c
      write(6,*) 'To which file do you want the output?'
      read(5,*) mfile
c
      open(ipoutf,file=mfile,status='new',iostat=iflag)
c
      if (iflag.ne.0) then
c
         write(6,*) 'The file ',mfile,'already exists.'
         goto 16
c
      endif
c
c-----------------------------------------------------------------------c
c
c     Input
c
c-----------------------------------------------------------------------c
c
      if (ynscrn.eq.1) write(6,*) 'Crack length a [mm] ?'
      read(ipinpf,*) a
      if (ynecho.eq.1) write(ipecho,1000) a
c
      if (ynscrn.eq.1) write(6,*) 'Damage radius rc ?'
```

```
      read(ipinpf,*) rc
      if (ynecho.eq.1) write(ipecho,1000) rc
c
      if (ynscrn.eq.1) write(6,*) 'Young's modulus E [MPa] ?'
      read(ipinpf,*) E
      if (ynecho.eq.1) write(ipecho,1000) E
c
      if (ynscrn.eq.1) write(6,*) 'Poisson's ratio nu ?'
      read(ipinpf,*) nu
      if (ynecho.eq.1) write(ipecho,1000) nu
c
      if (ynscrn.eq.1) write(6,*) 'With or without T-stress (1/0)?'
      read(ipinpf,*) Tyn
      if (ynecho.eq.1) write(ipecho,1300) Tyn
c
      if (ynscrn.eq.1) write(6,*) 'Starting crack angle,
     $end crack angle and interval ?'
      read(ipinpf,*) betas, betae, betai
      if (ynecho.eq.1) write(ipecho,1000) betas, betae, betai
c
c-----------------------------------------------------------------------c
c
c     Main program
c
c-----------------------------------------------------------------------c
c
      beta = betas
      j = 1
c
200   continue
c
      if (ynscrn.eq.1) write(6,*) 'Load stress sigma [MPa] ?'
      read(ipinpf,*) sigma
      if (ynecho.eq.1) write(ipecho,1000) sigma
c
      KI  = sigma*sqrt(pi*a)*sin(pi*beta/180.)**2
      KII = sigma*sqrt(pi*a)*sin(pi*beta/180.)*cos(pi*beta/180.)
c
      if (Tyn.eq.1) then
c
         T = sigma*cos(2.*pi*beta/180.)
         fact = 1.
c
      else
c
         T = 0.
         fact = sqrt(2.*pi*rc)
c
      endif
c
c     write(ipoutf,1100) KI,KII,T
c
      sitmax(j) = 0
c
      do 100, i = -180,180
c
         theta = pi*i/180.
c
         fxi  = cos(0.5*theta)*(1.-sin(0.5*theta)*sin(1.5*theta))
         fyi  = cos(0.5*theta)*(1.+sin(0.5*theta)*sin(1.5*theta))
         fxyi = cos(0.5*theta)*sin(0.5*theta)*cos(1.5*theta)
         fxii =-sin(0.5*theta)*(2.+cos(0.5*theta)*cos(1.5*theta))
         fyii = sin(0.5*theta)*cos(0.5*theta)*cos(1.5*theta)
         fxyii= cos(0.5*theta)*(1.-sin(0.5*theta)*sin(1.5*theta))
c
         KINOR  = KI/sqrt(2.*pi*rc)
         KIINOR = KII/sqrt(2.*pi*rc)
```

```
c
          sigmax = KINOR*fxi + KIINOR*fxii + T
          sigmay = KINOR*fyi + KIINOR*fyii
          tauxy  = KINOR*fxyi + KIINOR*fxyii
c
          sigmat = sigmax*sin(theta)**2 + sigmay*cos(theta)**2
     $           - 2.*tauxy*sin(theta)*cos(theta)
c
          if (sigmat.gt.sitmax(j)) then
c
             sitmax(j)  = sigmat
             themax = -theta*180./pi
c
          endif
c
100    continue
c
       write(ipoutf,1100) beta,sitmax(j)*fact,themax
c
       beta = beta + betai
       j = j + 1
c
       if (beta.lt.(betae+0.1)) goto 200
c
       do 300, k = 1, j-1
c
          sitmax(k)=sitmax(k)/sitmax(j-1)
          write(ipoutf,1100) beta,sitmax(k)*fact
c
300    continue
c
       stddev = 0.
c
       do 400, k = 1, j-1
c
          stddev = stddev + ( sitmax(k) - 1. )**2
c
400    continue
c
       write(ipoutf,1000) stddev
c
c-----------------------------------------------------------------------c
c
c      End Main program
c
c-----------------------------------------------------------------------c
c
1000   format(e12.5)
1100   format(e12.5,2x,e12.5,2x,e12.5)
1200   format(e12.5,2x,e12.5,2x,e12.5,2x,e12.5)
1300   format(e12.5,2x,e12.5,2x,e12.5,2x,e12.5,2x,e12.5)
c
       end
c
ccccccccccccccccccccccccccccccccccccccccccccccccccccccccccccccccccccc
c
```

Source code used to evaluate the hoop stresses σ_θ around a crack tip in an anisotropic plate

```
      program anitheta
ccccccccccccccccccccccccccccccccccccccccccccccccccccccccccccccccccccccc
c
c     Program to determine the propagation angle of a crack under
c     mixed mode I and II loading in an anisotropic plate
c
ccccccccccccccccccccccccccccccccccccccccccccccccccccccccccccccccccccccc
c
c     Variabels used to open the files
c
c-----------------------------------------------------------------------c
c
      integer           nmax
      parameter         (nmax=12)
c
      integer           ipinpf,ipoutf,ipecho
      integer           iflag
      integer           ynscrn,ynecho
      character*20      mfile,ifile,efile
      character*4       letter
      parameter         (ipoutf=8,ipecho=9)
c
c-----------------------------------------------------------------------c
c
c     Variabels used to open the plot window
c
c-----------------------------------------------------------------------c
c
      double precision sigma,pi,a,beta,theta
      double precision Ex,Ey,Gxy,nuyx,nuxy,re,ae
      double precision E,G,nu
      double precision KI,KII,T,fxi,fyi,fxyi,fxii,fyii,fxyii
      double precision KINOR,KIINOR,stddev
      double precision sigmax,sigmay,tauxy,sigmat,themax,rc
      double precision sxr,syr,txyr,sxal,syal,txyal,rotang
      double precision betas,betae,betai,sitmax(nmax)
      double complex    s1acc,s2acc,s1,s2,phi1,phi2,c1
      double complex    im,betar
      integer           i,Tyn,Lamyn,j,k
c
      data pi           / 3.141592654 /
c
c-----------------------------------------------------------------------c
c
c     Input from screen or file
c
c-----------------------------------------------------------------------c
c
      write(6,*) 'Input from the screen or from a file (s/f)?'
      read(5,*) letter
c
      if (letter.eq.'f') then
c
         ipinpf = 7
         ynscrn = 0
         ynecho   = 0
c
14       continue
c
         write(6,*) 'Type the input-full file naam:'
         read(5,*) ifile
c
         open(ipinpf,file=ifile,status='old',iostat=iflag)
c
```

```
         if (iflag.ne.0) then
c
            write(6,*) 'The file ',ifile,'doesn't exists.'
            goto 14
c
         endif
c
      else
c
         ipinpf = 5
         ynscrn = 1
         ynecho   = 0
c
         write(6,*) 'Do you want an echo-file of the input (y/n)?'
         read(5,*) letter
c
         if (letter.eq.'y') then
c
            ynecho = 1
c
15          continue
c
            write(6,*) 'Type the full echo-file naam:'
            read(5,*) efile
c
            open(ipecho,file=efile,status='new',iostat=iflag)
c
            if (iflag.ne.0) then
c
               write(6,*) 'The file ',efile,'already exists.'
               goto 15
c
            endif
c
         endif
c
      endif
c
c-----------------------------------------------------------------------c
c
c     Output to outf file
c
c-----------------------------------------------------------------------c
c
16    continue
c
      write(6,*) 'To which file do you want the output?'
      read(5,*) mfile
c
      open(ipoutf,file=mfile,status='new',iostat=iflag)
c
      if (iflag.ne.0) then
c
         write(6,*) 'The file ',mfile,'already exists.'
         goto 16
c
      endif
c
c-----------------------------------------------------------------------c
c
c     Input
c
c-----------------------------------------------------------------------c
c
      if (ynscrn.eq.1) write(6,*) 'Crack length a [mm] ?'
      read(ipinpf,*) a
```

```
      if (ynecho.eq.1) write(ipecho,1200) a
c
      if (ynscrn.eq.1) write(6,*) 'Damage radius rc ?'
      read(ipinpf,*) rc
      if (ynecho.eq.1) write(ipecho,1000) rc
c
      if (ynscrn.eq.1) write(6,*) 'Young's modulus Ex [MPa] ?'
      read(ipinpf,*) Ex
      if (ynecho.eq.1) write(ipecho,1200) Ex
c
      if (ynscrn.eq.1) write(6,*) 'Young's modulus Ey [MPa] ?'
      read(ipinpf,*) Ey
      if (ynecho.eq.1) write(ipecho,1200) Ey
c
      if (ynscrn.eq.1) write(6,*) 'Shear modulus Gxy [MPa] ?'
      read(ipinpf,*) Gxy
      if (ynecho.eq.1) write(ipecho,1200) Gxy
c
      if (ynscrn.eq.1) write(6,*) 'Poisson's ratio nuyx ?'
      read(ipinpf,*) nuyx
      if (ynecho.eq.1) write(ipecho,1100) nuyx
c
      if (ynscrn.eq.1) write(6,*) 'Young's modulus E [MPa] ?'
      read(ipinpf,*) E
      if (ynecho.eq.1) write(ipecho,1200) E
c
      if (ynscrn.eq.1) write(6,*) 'Poisson's ratio nu ?'
      read(ipinpf,*) nu
      if (ynecho.eq.1) write(ipecho,1100) nu
c
      if (ynscrn.eq.1) write(6,*) 'With or without T-stress (1/0)?'
      read(ipinpf,*) Tyn
      if (ynecho.eq.1) write(ipecho,1300) Tyn
c
      if (ynscrn.eq.1) write(6,*) 'Laminate or homogeneous (1/0)?'
      read(ipinpf,*) Lamyn
      if (ynecho.eq.1) write(ipecho,1300) Lamyn
c
      if (ynscrn.eq.1) write(6,*) 'Starting crack angle,' ,
     $' end crack angle and interval ?'
      read(ipinpf,*) betas, betae, betai
      if (ynecho.eq.1) write(ipecho,1200) betas, betae, betai
c
c-----------------------------------------------------------------------c
c
c     Main program
c
c-----------------------------------------------------------------------c
c
      G = E/(2.*(1.+nu))
      nuxy = nuyx*Ex/Ey
      re = sqrt(Ex/Ey)
      ae = (0.5*Ex/Gxy)-nuxy
      im = (0.,1.)
c
      s1acc = cmplx( sqrt(0.5*cmplx(re-ae)))
     $      + im*cmplx(sqrt(0.5*cmplx(re+ae)))
      s2acc = cmplx(-sqrt(0.5*cmplx(re-ae)))
     $      + im*cmplx(sqrt(0.5*cmplx(re+ae)))
c
      beta = betas
      j =  1
c
200   continue
c
      if (ynscrn.eq.1) write(6,*) 'Load stress sigma [MPa] ?'
      read(ipinpf,*) sigma
```

```
      if (ynecho.eq.1) write(ipecho,1000) sigma
c
      betar = cmplx((90.-beta)*pi/180.)
c
      s1 = (s1acc*cos(betar)-sin(betar))
     $   / (cos(betar)+s1acc*sin(betar))
      s2 = (s2acc*cos(betar)-sin(betar))
     $   / (cos(betar)+s2acc*sin(betar))
c
      KI  = sigma*sqrt(pi*a)*sin(pi*beta/180.)**2
      KII = sigma*sqrt(pi*a)*sin(pi*beta/180.)*cos(pi*beta/180.)
c
      if (Tyn.eq.1) then
c
         T = sigma*(cos(pi*beta/180.)**2
     $     + sin(pi*beta/180.)**2*real(s1*s2)
     $     + sin(pi*beta/180.)*cos(pi*beta/180.)*real(s1+s2) )
c
      else
c
         T = 0.
c
      endif
c
      write(ipoutf,1000) KI,KII,T,s1,s2
c
      sitmax(j) = 0.
c
      do 100, i = -180,180
c
         theta = pi*i/180.
c
         phi1 = sqrt( cmplx( cos(theta) ) + s1*cmplx( sin(theta) ) )
         phi2 = sqrt( cmplx( cos(theta) ) + s2*cmplx( sin(theta) ) )
         c1   = (1.,0.)
c
         fxi  =-real( ((s1*s2)/(s1-s2)) * ((s1/phi1)-(s2/phi2)) )
         fxii =-real( (c1/(s1-s2)) * ((s1**2/phi1)-(s2**2/phi2)) )
         fyi  =-real( (c1/(s1-s2)) * ((s2/phi1)-(s1/phi2)) )
         fyii =-real( (c1/(s1-s2)) * ((c1/phi1)-(c1/phi2)) )
         fxyi = real( ((s1*s2)/(s1-s2)) * ((c1/phi1)-(c1/phi2)) )
         fxyii= real( (c1/(s1-s2)) * ((s1/phi1)-(s2/phi2)) )
c
         KINOR = KI/sqrt(2.*pi*rc)
         KIINOR= KII/sqrt(2.*pi*rc)
c
         sigmax = KINOR*fxi + KIINOR*fxii + T
         sigmay = KINOR*fyi + KIINOR*fyii
         tauxy  = KINOR*fxyi+ KIINOR*fxyii
c
c-----------------------------------------------------------------------c
c
         if (Lamyn.eq.1) then
c
            rotang = - pi*(90.-beta)/180.
c
            sxr    = sigmax*cos(rotang)**2 + sigmay*sin(rotang)**2
     $             + 2.*tauxy*sin(rotang)*cos(rotang)
            syr    = sigmax*sin(rotang)**2 + sigmay*cos(rotang)**2
     $             - 2.*tauxy*sin(rotang)*cos(rotang)
            txyr   = - sigmax*cos(rotang)*sin(rotang)
     $             + sigmay*sin(rotang)*cos(rotang)
     $             + tauxy*(cos(rotang)**2-sin(rotang)**2)
c
            sxal = ((E/(1.-nu**2.))*(1.-nuxy*nu)*sxr/Ex)
     $           + ((E/(1.-nu**2.))*(nu-nuyx)*syr/Ey)
```

```
            syal = ((E/(1.-nu**2.))*(nu-nuxy)*sxr/Ex)
     $           + ((E/(1.-nu**2.))*(1.-nuyx*nu)*syr/Ex)
            txyal= txyr*G/Gxy
c
            sigmat = sxal*sin(theta-rotang)**2
     $             + syal*cos(theta-rotang)**2
     $             - 2.*txyal*sin(theta-rotang)*cos(theta-rotang)
c
         else
c
            sigmat = sigmax*sin(theta)**2 + sigmay*cos(theta)**2
     $             - 2.*tauxy*sin(theta)*cos(theta)
c
         endif
c
c-----------------------------------------------------------------------c
c
         if (sigmat.gt.sitmax(j)) then
c
            sitmax(j) = sigmat
            themax    = -theta*180./pi
c
         endif
c
100   continue
c
      write(ipoutf,1000) beta,sitmax(j),themax
c
      beta = beta + betai
      j = j + 1
c
      if (beta.lt.(betae+0.1)) goto 200
c
      do 300, k = 1, j-1
c
         sitmax(k)=sitmax(k)/sitmax(j-1)
         write(ipoutf,1100) beta,sitmax(k)
c
300   continue
c
      stddev = 0.
c
      do 400, k = 1, j-1
c
         stddev = stddev + ( sitmax(k) - 1. )**2
c
400   continue
c
      write(ipoutf,1000) stddev
c
c-----------------------------------------------------------------------c
c
c     End Main program
c
c-----------------------------------------------------------------------c
c
1000  format(e12.5,7(2x,e12.5))
1100  format(f12.5,7(2x,f12.5))
1200  format(f12.0,7(2x,f12.0))
1300  format(i5,7(2x,i5))
c
      end
c
ccccccccccccccccccccccccccccccccccccccccccccccccccccccccccccccccccccccc
c
```

Source code used to evaluate the energy density around a crack tip in an isotropic plate

```
      program isotheo
ccccccccccccccccccccccccccccccccccccccccccccccccccccccccccccccccccccccc
c
c     Program to determine the propagation angle of a crack under
c     mixed mode I and II loading
c
ccccccccccccccccccccccccccccccccccccccccccccccccccccccccccccccccccccccc
c
      integer           nmax
      parameter         (nmax=10)
c
c-----------------------------------------------------------------------c
c
c     Variabels used to open the files
c
c-----------------------------------------------------------------------c
c
      integer           ipinpf,ipoutf,ipecho
      integer           iflag
      integer           ynscrn,ynecho
      character*20      mfile,ifile,efile
      character*4       letter
      parameter         (ipoutf=8,ipecho=9)
c
c-----------------------------------------------------------------------c
c
c     Variabels used to open the plot window
c
c-----------------------------------------------------------------------c
c
      double precision sigma,pi,a,beta,theta,sigma0,E,G,nu
      double precision KI,KII,T,theta0,fx,fy,fxy
      double precision TDNOR1,TDNOR2,TDNOR3,TD0,KINOR1,KINOR2
      double precision sigmax,sigmay,tauxy,Td,Tv,Ttot,Tdcon
      double precision Tvmax(nmax),Tvthmx
      double precision betas,betae,betai,stddev
      integer           i,j,Tyn,k
c
      data pi           / 3.141592654 /
c
c-----------------------------------------------------------------------c
c
c     Input from screen or file
c
c-----------------------------------------------------------------------c
c
      write(6,*) 'Input from the screen or from a file (s/f)?'
      read(5,*) letter
c
      if (letter.eq.'f') then
c
         ipinpf = 7
         ynscrn = 0
         ynecho   = 0
c
14       continue
c
         write(6,*) 'Type the input-full file naam:'
         read(5,*) ifile
c
         open(ipinpf,file=ifile,status='old',iostat=iflag)
c
         if (iflag.ne.0) then
c
```

```
            write(6,*) 'The file ',ifile,'doesn't exists.'
            goto 14
c
         endif
c
      else
c
         ipinpf = 5
         ynscrn = 1
         ynecho   = 0
c
         write(6,*) 'Do you want an echo-file of the input (y/n)?'
         read(5,*) letter
c
         if (letter.eq.'y') then
c
            ynecho = 1
c
15          continue
c
            write(6,*) 'Type the full echo-file naam:'
            read(5,*) efile
c
            open(ipecho,file=efile,status='new',iostat=iflag)
c
            if (iflag.ne.0) then
c
               write(6,*) 'The file ',efile,'already exists.'
               goto 15
c
            endif
c
         endif
c
      endif
c
c-----------------------------------------------------------------------c
c
c     Output to outf file
c
c-----------------------------------------------------------------------c
c
16    continue
c
      write(6,*) 'To which file do you want the output?'
      read(5,*) mfile
c
      open(ipoutf,file=mfile,status='new',iostat=iflag)
c
      if (iflag.ne.0) then
c
         write(6,*) 'The file ',mfile,'already exists.'
         goto 16
c
      endif
c
c-----------------------------------------------------------------------c
c
c     Input
c
c-----------------------------------------------------------------------c
c
      if (ynscrn.eq.1) write(6,*) 'Crack length a [mm] ?'
      read(ipinpf,*) a
      if (ynecho.eq.1) write(ipecho,1000) a
c
      if (ynscrn.eq.1) write(6,*) 'Yield stress sigma0 [MPa] ?'
```

```
      read(ipinpf,*) sigma0
      if (ynecho.eq.1) write(ipecho,1000) sigma0
c
      if (ynscrn.eq.1) write(6,*) 'Young's modulus E [MPa] ?'
      read(ipinpf,*) E
      if (ynecho.eq.1) write(ipecho,1000) E
c
      if (ynscrn.eq.1) write(6,*) 'Poisson's ratio nu ?'
      read(ipinpf,*) nu
      if (ynecho.eq.1) write(ipecho,1000) nu
c
      if (ynscrn.eq.1) write(6,*) 'With or without T-stress (1/0)?'
      read(ipinpf,*) Tyn
      if (ynecho.eq.1) write(ipecho,1050) Tyn
c
      if (ynscrn.eq.1) write(6,*) 'Starting crack angle',
     $' end crack angle and interval ?'
      read(ipinpf,*) betas, betae, betai
      if (ynecho.eq.1) write(ipecho,1100) betas, betae, betai
c
c-----------------------------------------------------------------------c
c
c     Main program
c
c-----------------------------------------------------------------------c
c
      G = E/(2.*(1+nu))
c
      beta = betas
      j = 1
c
200   continue
c
      if (ynscrn.eq.1) write(6,*) 'Load stress sigma [MPa] ?'
      read(ipinpf,*) sigma
      if (ynecho.eq.1) write(ipecho,1000) sigma
c
      KI  = sigma*sqrt(pi*a)*sin(pi*beta/180.)**2
      KII = sigma*sqrt(pi*a)*sin(pi*beta/180.)*cos(pi*beta/180.)
c
      if (Tyn.eq.1) then
c
         T = sigma*cos(2.*pi*beta/180.)
c
      else
c
         T = 0.
c
      endif
c
      theta0 = -2.*KII/KI
c
      Tvmax(j) = 0
c
      do 100, i = -180,180
c
         theta = pi*i/180.
c
         fx  = cos(0.5*theta)*(1.-sin(0.5*theta)*sin(1.5*theta))
     $       - 0.5*theta0
     $       * (-sin(0.5*theta)*(2.+cos(0.5*theta)*cos(1.5*theta)))
         fy  = cos(0.5*theta)*(1.+sin(0.5*theta)*sin(1.5*theta))
     $       - 0.5*theta0
     $       * (sin(0.5*theta)*cos(0.5*theta)*cos(1.5*theta))
         fxy = cos(0.5*theta)*sin(0.5*theta)*cos(1.5*theta)
     $       - 0.5*theta0
```

```
     $       * (cos(0.5*theta)*(1.-sin(0.5*theta)*sin(1.5*theta)))
c
c         write(ipoutf,1200) theta,fx,fy,fxy
c
          TDNOR1 = (1/(6.*G))*((fx-fy)**2+fx*fy+3*fxy**2)
          TDNOR2 = ((2.*T*fx)-T*fy)/(6.*G)
          TDNOR3 = T**2/(6.*G)
          TD0    = sigma0**2/(6.*G)
c
          KINOR1 = (-TDNOR2+SQRT(TDNOR2**2-4.*TDNOR1*(TDNOR3-TD0)))
     $           / (2.*(TDNOR1))
          KINOR2 = (-TDNOR2-SQRT(TDNOR2**2-4.*TDNOR1*(TDNOR3-TD0)))
     $           / (2.*(TDNOR1))
c
          sigmax = KINOR1*fx+T
          sigmay = KINOR1*fy
          tauxy  = KINOR1*fxy
c
c         write(ipoutf,1200) theta,sigmax,sigmay,tauxy
c
          Td   = TDNOR1*KINOR1**2 + TDNOR2*KINOR1 + TDNOR3
          Tv   = ((1-2.*nu)/((6.*G)*(2.+2.*nu)))*(sigmax+sigmay)**2
          Ttot = (1./(4.*G*(1.+nu)))
     $         * (sigmax**2+sigmay**2-2.*nu*sigmax*sigmay
     $         + 2.*(1.+nu)*tauxy**2)
          Tdcon = (1./(6.*G))
     $          * (sigmax**2+sigmay**2-sigmax*sigmay+3.*tauxy**2)
c
          if (Tv.gt.Tvmax(j)) then
c
             Tvmax(j)  = Tv
             Tvthmx = -theta*180./pi
c
          endif
c
c         write(ipoutf,1300) theta,Tv,Td,Ttot,Tv/Td
c
100    continue
c
c      write(ipoutf,*)
       write(ipoutf,1100) beta,Tvmax(j),Tvthmx
c      write(ipoutf,*)
c
       beta = beta + betai
       j = j + 1
c
       if (beta.lt.(betae+0.1)) goto 200
c
       do 300, k = 1, j-1
c
          Tvmax(k)=Tvmax(k)/Tvmax(j-1)
          write(ipoutf,1100) beta,Tvmax(k)
c
300    continue
c
       stddev = 0.
c
       do 400, k = 1, j-1
c
          stddev = stddev + ( Tvmax(k) - 1. )**2
c
400    continue
c
       write(ipoutf,1000) stddev
c
c------------------------------------------------------------------c
c
```

```
c      End Main program
c
c-----------------------------------------------------------------------c
c
1000   format(e12.5)
1050   format(i5)
1100   format(e12.5,2x,e12.5,2x,e12.5)
1200   format(e12.5,2x,e12.5,2x,e12.5,2x,e12.5)
1300   format(e12.5,2x,e12.5,2x,e12.5,2x,e12.5,2x,e12.5)
c
       end
c
ccccccccccccccccccccccccccccccccccccccccccccccccccccccccccccccccccccc
c
```